

12-2020

A Pharmacological Strategy Against African Sleeping Sickness

Wahaj Zuberi

Follow this and additional works at: https://digitalcommons.library.tmc.edu/utgsbs_dissertations



Part of the [Microbiology Commons](#)

Recommended Citation

Zuberi, Wahaj, "A Pharmacological Strategy Against African Sleeping Sickness" (2020). *The University of Texas MD Anderson Cancer Center UTHealth Graduate School of Biomedical Sciences Dissertations and Theses (Open Access)*. 1045.

https://digitalcommons.library.tmc.edu/utgsbs_dissertations/1045

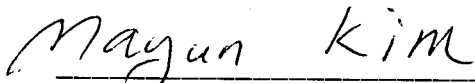
This Thesis (MS) is brought to you for free and open access by the The University of Texas MD Anderson Cancer Center UTHealth Graduate School of Biomedical Sciences at DigitalCommons@TMC. It has been accepted for inclusion in The University of Texas MD Anderson Cancer Center UTHealth Graduate School of Biomedical Sciences Dissertations and Theses (Open Access) by an authorized administrator of DigitalCommons@TMC. For more information, please contact digitalcommons@library.tmc.edu.

A PHARMACOLOGICAL STRATEGY AGAINST AFRICAN SLEEPING SICKNESS

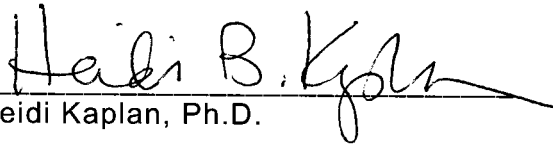
By

Wahaj Zuberi, B.S.

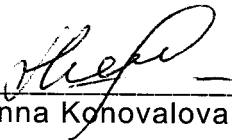
APPROVED:



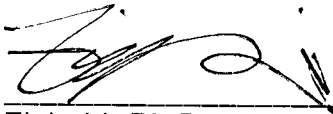
Nayun Kim, Ph.D.
Advisory Professor



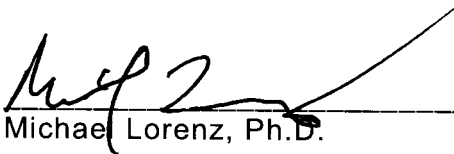
Heidi Kaplan, Ph.D.



Anna Konovalova, Ph.D.



Ziyin Li, Ph.D.



Michael Lorenz, Ph.D.

APPROVED:

Dean, The University of Texas
MD Anderson Cancer Center UTHealth Graduate School of Biomedical Sciences

A PHARMACOLOGICAL STRATEGY AGAINST AFRICAN SLEEPING SICKNESS

A

THESIS

Presented to the Faculty of

The University of Texas

MD Anderson Cancer Center

UTHealth Graduate School of Biomedical Sciences

in Partial Fulfillment

of the Requirements

for the Degree of

MASTER OF SCIENCE

By

Wahaj Zuberi, B.S.

Houston, Texas

December 2020

To my family and friends.

Acknowledgements

Firstly, I would like to thank my advisor, Dr. Nayun Kim. At the start of graduate school, she was the only one who reached out to me and took interest in having me join her lab. I know I am not the greatest student, but I am thankful for her patience and guidance throughout my journey of pursuing my master's degree. I have learned a lot from her, and I look forward to furthering my growth as a scientist.

Thank you to all my colleagues, Allie, Shivani, Duy, and Kasey, who I am also happy to call my good friends. When I started graduate school and joined the lab, it was a bit scary for me, but who knew I would meet such great people to make my time here fun and cheerful. Thank you all for always answering my questions, no matter how silly they were, for always taking the time to teach me something new and providing feedback, and for always encouraging me and making it all worthwhile.

Lastly, thank you to my committee members, Drs. Heidi Kaplan, Anna Konovalova, Ziyin Li, and Michael Lorenz. Your words of encouragement and reassurance during committee meetings were a huge relief. It was nice to know that such qualified credible scientists approved of what I was doing, and I appreciated the time you all took to help me out and provide feedback.

This master's journey for me has been a pretty fun one. I faced many new challenges and I somehow have managed to make it out to the other side. I am looking forward to the next big chapters in my life and am looking forward to sharing with everyone what I will achieve in the future.

A PHARMACOLOGICAL STRATEGY AGAINST AFRICAN SLEEPING SICKNESS

Wahaj Zuberi, B.S.

Advisory Professor: Nayun Kim, Ph.D.

Trypanosoma brucei is a parasitic eukaryote and is the causal agent of the disease known as African sleeping sickness, transmitted via the bite of a tsetse fly. If left untreated, the parasite ultimately crosses the blood-brain barrier eventually leading to death. Currently there are five approved drugs used to treat it, each with toxic side effects and effective at specific disease stages. A more effective and less toxic drug candidate is highly sought after. The essential enzyme, dUTPase, may be an excellent drug target in the parasite and can be tested utilizing *S. cerevisiae* as a model system.

dUTPase is essential in *T. brucei* (tbdUTPase), yeast (yDut1), and humans (hDUT). dUTPase being a dimer in *T. brucei*, but a trimer in yeast and humans, we hypothesize there may be a molecule that inhibits the function of tbdUTPase, but not of yDut1 and hDUT. The endogenous yDut1 was knocked down via auxin inducible degron system in order to complement its loss by transforming plasmids containing human and *T. brucei* dUTPase genes. Induced expression of hDUT and tbdUTPase did not seem to complement the loss of yDut1. As an alternative strategy, the dUTPase genes from human and *T. brucei* were next integrated into the yeast genome at the inactive *HO* locus. The results of this experiment were inconclusive and remain to be further explored.

In order to identify a small molecule ligand of tbdUTPase, a high throughput virtual drug screen was performed through Schrödinger's Suite. This led to the discovery of 13 molecules that bind to tbdUTPase but not to hDUT. Out of the 13, one molecule showed cytotoxic effects against the parasite but not against yeast.

To determine if the single molecule found was dUTPase specific, yDut1, hDUT, and tbdUTPase proteins were purified and their enzymatic activity was measured in the presence of the single molecule. The results indicated that the molecule found to have cytotoxic effect against *T. brucei* cells was not dUTPase specific. Although the results do not support the initial hypothesis, the dUTPase pathway, as well as virtual drug screening hold promise and require further research.

Table of Contents

Approval Sheet	i
Title Page	ii
Dedication	iii
Acknowledgments	iv
Abstract	v
Table of Contents	vii
List of Figures	ix
List of Tables	x
Chapter 1: Introduction	1
1. African Sleeping Sickness.....	2
2. dUTPase/Uracil in the DNA.....	5
3. Auxin Inducible Degron System.....	10
4. High Throughput Virtual Screen for dUTPase ligands.....	12
Chapter 2: Materials and Methods	14
1. Yeast Strains and Plasmids.....	15
2. Auxin Growth Assay.....	17
3. Auxin Growth Curves.....	17
4. High Throughput Virtual Screen using Schrödinger's Suite.....	18
5. <i>T. brucei</i> /Yeast Growth Curve.....	18
6. Protein Purification.....	19
7. Western Immunoblotting.....	21
8. Pyrophosphate-based Enzymatic Activity.....	21
9. PCR-based Enzymatic Activity.....	22
Chapter 3: Results	23
1. Auxin growth assay/curves showing growth inhibition in the presence of auxin.....	24

2. Expression of human and <i>T. brucei</i> dUTPase in yeast.....	37
3. High Throughput Virtual Screen for <i>T. brucei</i> dUTPase ligands using Schrödinger's suite.....	51
4. <i>T. brucei</i> /yeast viability testing with molecules found from the High Throughput Virtual Screen.....	58
5. Overexpression and purification of yeast, human, and <i>T. brucei</i> dUTPase proteins.....	62
6. Enzymatic activity of dUTPase proteins.....	66
Chapter 4: Discussion.....	61
Bibliography.....	67

List of Figures

Figure 1: Uracil (dUTP) can be incorporated into DNA.....	6
Figure 2: Uracil mediated DNA damage.....	8
Figure 3: Auxin inducible degron system.....	11
Figure 4: dUTPase crystal structures.....	25
Figure 5: Spot growth assay with and without auxin.....	31
Figure 6: Growth curves showing effectiveness of AID system.....	32
Figure 7: Degradation of Dut1 in YNK425.....	34
Figure 8: dTTP synthesis pathway and the targets of auxin, 5-FU, and MTX.....	36
Figure 9: General structure of plasmids containing yeast, human, and <i>T. brucei</i> dUTPase genes.....	39
Figure 10: Assay testing functional complementation following yeast transformation.....	41
Figure 11: Western blot showing expression of HA tagged hDUT and tbdUTPase proteins.....	44
Figure 12: Growth curves testing functional complementation of hDUT and tbdUTPase genes integrated into the yeast genome in the <i>HO</i> gene.....	46
Figure 13: Growth curves showing growth behavior of inactive tbdUTPase integrated into the <i>HO</i> gene.....	48
Figure 14: Western blot tracking the degradation of endogenous yDUT1-AID.....	50
Figure 15: <i>T. brucei</i> dUTPase residues interacting with dUMP.....	52
Figure 16: HTVS result showing positive binding hits for <i>T. brucei</i> dUTPase.....	55
Figure 17: Growth curves testing the effect of molecules 1-13 on <i>T. brucei</i>	60
Figure 18: Growth curves testing the effect of molecules 1-13 on YNK421.....	61
Figure 19: Protein staining results of collected fractions and elution.....	63
Figure 20: Final protein staining image of purified proteins.....	65
Figure 21: PCR-based dUTPase enzymatic activity assay.....	70

List of Tables

Table 1: Plasmids and yeast strains.....	15
Table 2: Auxin CFU assay showing survival rates of YNK421 and YNK425.....	27
Table 3: Auxin CFU assay showing survival rates of YNK425 and YNK684.....	29
Table 4: dUTPase gene sequences for yeast, human, and <i>T. brucei</i>	38
Table 5: CFU assay of YNK425 transformed with vector, yDUT1, hDUT, and tbdUTPase plasmids.....	40
Table 6: Thirteen molecules narrowed down by HTVS.....	56
Table 7: Protein concentrations of purified proteins.....	65
Table 8: PiPer Pyrophosphate assay.....	67

Chapter 1: Introduction

1.1 African Sleeping Sickness

Human African trypanosomiasis, or African sleeping sickness, is an infectious disease caused by the parasitic eukaryote *Trypanosoma brucei*. Transmitted by the bite of a tsetse fly, this disease is a significant problem and restricted to the sub-Saharan region of Africa [1]. There are two pathogenic subspecies of *T. brucei*: 1) *T. b. gambiense* is the causal agent of Western African sleeping sickness, responsible for over 90% of sleeping sickness cases, and causes chronic sleeping sickness; 2) *T. b. rhodesiense* is the causal agent of Eastern African sleeping sickness and causes more acute sleeping sickness [2].

There are two stages to the disease, the first is called the hemo-lymphatic stage, in which the parasite is present in the bloodstream and lymphatic system, and the second is called the meningo-encephalitic stage where the parasite has crossed the blood-brain barrier resulting in neurological damage [1]. Ultimately if left untreated, patients gradually progress into a coma followed by possible organ failure and finally death. Rhodesiense sleeping sickness progresses faster with death resulting within months, whereas death with Gambiense sleeping sickness can take years [3]. The signs and symptoms of the disease caused by the two subspecies are overall the same. In the first stage of the disease, the leading and most common symptoms include fever, headaches, weakness, pruritus, lymphadenopathy, and in some cases hepatosplenomegaly. In the second stage of the disease, sleeping disorder is the primary symptom followed by neurological symptoms, such as various movement and speech disorders [1]. This disease often also has the risk of being misdiagnosed due to similarities with other fever-causing and neuropsychiatric diseases/problems.

Diagnosing African sleeping sickness is a two-stage process: screening followed by diagnostic confirmation [2]. The best test in terms of practicality and speed to diagnose African sleeping sickness is by the card agglutination test for

trypanosomiasis (CATT). This is a serological test that detects trypanosome-specific antibody in blood, plasma, or serum and the agglutination reaction is then analyzed visually [1, 4]. Other serological and molecular assays are available; however, they are to be analyzed with caution due to lack of personnel training, laboratory testing facilities, and poor accuracy and reproducibility [5]. Positive results from these methods require further validation. The best method for confirmation is microscopic examination of the lymph node aspirate, blood, or cerebral spinal fluid for the presence of the parasite [1].

Development of a proper and viable treatment against the parasite has been difficult and unfeasible due to the presence of approximately 2000 variant surface glycoproteins (VSG) [1]. When infection initially occurs, the initial surface glycoproteins are recognized by the host immune system, leading to the production of appropriate antibodies. These antibodies are able to combat the presence of the parasite; however, the parasite is simultaneously changing its surface glycoprotein, so that it is no longer affected by the initial antibodies [6]. This cycle repeats itself ultimately leading to the host's immune system being unable to eliminate trypanosome [7]. Currently there are five drugs that are routinely used against African sleeping sickness: pentamidine and suramin are used to treat first-stage disease, and melarsoprol, eflornithine, and nifurtimox are used to treat the second-stage disease [5]. Diagnosis and treatment using first-stage drugs as early as possible are vital to increase the chance of a patient being cured. The drugs effective against the second stage of the disease run a significantly higher risk of toxic side effects, due to a greater level of complexity in administration, since it is necessary for them to cross the blood-brain barrier [5].

Treatment for African sleeping sickness is variable based on the stage of the disease and the subspecies that has infected the patient [8]. For *T. b. gambiense*, pentamidine is effective in the first stage of disease and eflornithine in combination

with nifurtimox is effective in the second stage of disease. For *T. b. rhodesiense*, suramin is effective in the first stage of disease and melarsoprol is effective in the second stage of disease.

For *T. b. gambiense*, the first choice of treatment is pentamidine [1, 5, 9]. Pentamidine is administered intramuscularly once daily over a span of 7 days, but can also be given intravenously, if diluted in saline beforehand. When administered, it is also followed by the administration of sugar, as hypoglycemia is one of the adverse side effects of the drug. In addition, other effects include pain and swelling at the injection site, hypotension, and gastrointestinal problems. Eflornithine is the first choice of treatment for patients for whom the disease has progressed to the second stage. More recently, eflornithine has been administered in combination with a second drug called nifurtimox. This nifurtimox-eflornithine combination therapy (NECT) has been shown to have higher cure rates along with lower fatality rates and less severe adverse effects [5]. Eflornithine is given as a monotherapy if nifurtimox is unavailable. With a complete NECT kit, nifurtimox is administered orally and eflornithine is administered intravenously. In combination, nifurtimox is given to the patient for ten days with three doses each day and eflornithine is given every twelve hours. If only eflornithine is administered, four infusions are given daily for fourteen days. For the NECT treatment, common side effects are abdominal pain, nausea, and headaches, whereas when eflornithine is given as a monotherapy side effects are more severe, leading to pruritus, diarrhea, myelosuppression, and even seizures [1, 5, 9].

For *T. b. rhodesiense*, the first choice of treatment is the drug suramin [10]. Suramin rapidly deteriorates once it is diluted and needs to be administered to the patient immediately intravenously. This drug is more complex to administer, since it requires a schedule, that varies with each patient and can require treatments for up to one month. In addition, it requires a test dose to avoid the risk of hypersensitivity

reactions [5]. Adverse side for suramin effects are typically mild and reversible including nephrotoxicity, neuropathy, agranulocytosis, and thrombocytopenia [1]. Melarsoprol is the final choice of treatment for patients who have progressed to the second stage of the disease. Melarsoprol is the most toxic drug out of the five that have been mentioned and is restricted to only be used for treating second stage T. b. rhodesiense disease [11]. The most important severe side effect as a result of melarsoprol treatment, administered intravenously every day for ten days, is an encephalopathic syndrome that leads to the death in majority of patients who are diagnosed with it. Patients are closely monitored to avoid progression of the encephalopathic syndrome [1, 5].

1.2 dUTPase/Uracil in DNA

There are many different mechanisms by which DNA modifications can occur through exogenous and endogenous damaging factors. One form of endogenous DNA modification is the incorporation of uracil into DNA [12]. Uracil can appear in DNA through two different methods, 1) cytosine deamination and 2) uracil incorporation into DNA instead of thymine during DNA replication/repair [13].

The rate of cytosine deamination is greatly increased when DNA is single-stranded, such as during DNA replication [14]. The newly incorporated uracil create premutagenic U:G mispairs. This can result in a transition from C:G to T:A since DNA polymerase effectively and efficiently incorporates adenine that pairs with the uracil and this is followed by the removal of uracil and incorporation of thymine in its place [15-17]. It has been calculated that cytosine deamination occurs in approximately 70 to 200 cytosine base pairs per day in every human cell [17]. Cytosines in different forms, such as in cyclobutene dimers are deaminated faster than other cytosines. Cytosine can also be deaminated enzymatically by enzymes, such as activation-induced deaminase, which has been suggested to target C:G base pairs directly [16].

The other source of uracil incorporation into DNA is through the normal function of eukaryotic DNA polymerase [7]. Deoxyuridine triphosphate (dUTP) is incorporated into DNA rather than deoxythymidine triphosphate (dTTP). DNA polymerases cannot distinguish between uracil and thymine base pairs, therefore uracil is freely incorporated into DNA rather than the appropriate thymine base pairs, depending on the available ratio of [dUTP/dTTP] (Figure 1) [7]. This however, results in stable U:A base pairing, which are not mutagenic, in contrast to the cytosine deamination which results in highly mutagenic U:G mispairs [18].

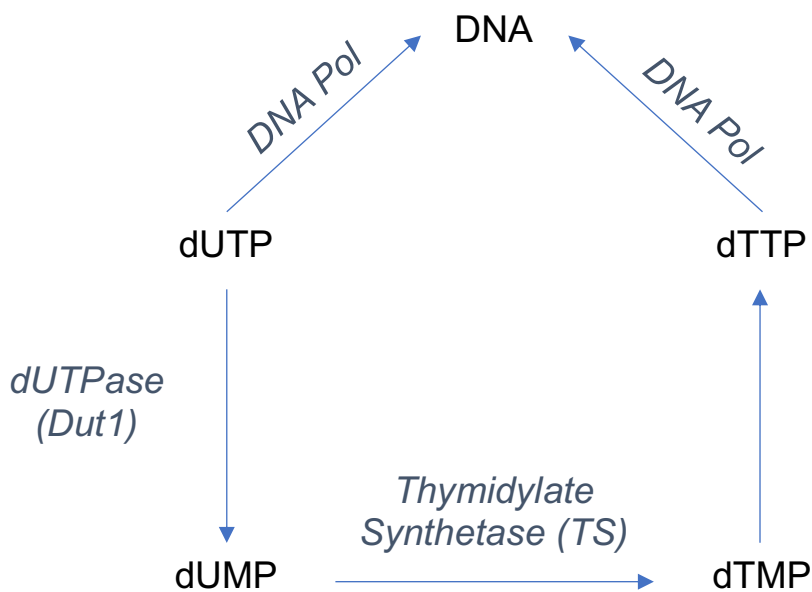


Figure 1: Uracil (dUTP) can be incorporated into DNA.

Both dUTP and dTTP can be incorporated into DNA via DNA Polymerase. The presence of dUTPase lowers [dUTP/dTTP] leading to greater synthesis of dTTP.

The thymidine synthesis pathway is the only pathway for the synthesis of thymine to be used during DNA replication via DNA polymerase [19]. Deoxyuridine triphosphate diphosphatase (dUTPase), Dut1 in *S. cerevisiae*, is an essential enzyme that hydrolyzes dUTP to deoxyuridine monophosphate (dUMP), a substrate for dTTP synthesis via other downstream enzymes to be used for appropriate DNA replication. This regulates the extent of uracil being incorporated into the DNA. Uracil in DNA is the cause of major mutations, in yeast, which ultimately lead to thymine-less cell death (**Figure 2**) [20, 21]. This occurs due to the increased [dUTP/dTTP] ratio, allowing for an increased direct incorporation by DNA polymerase.

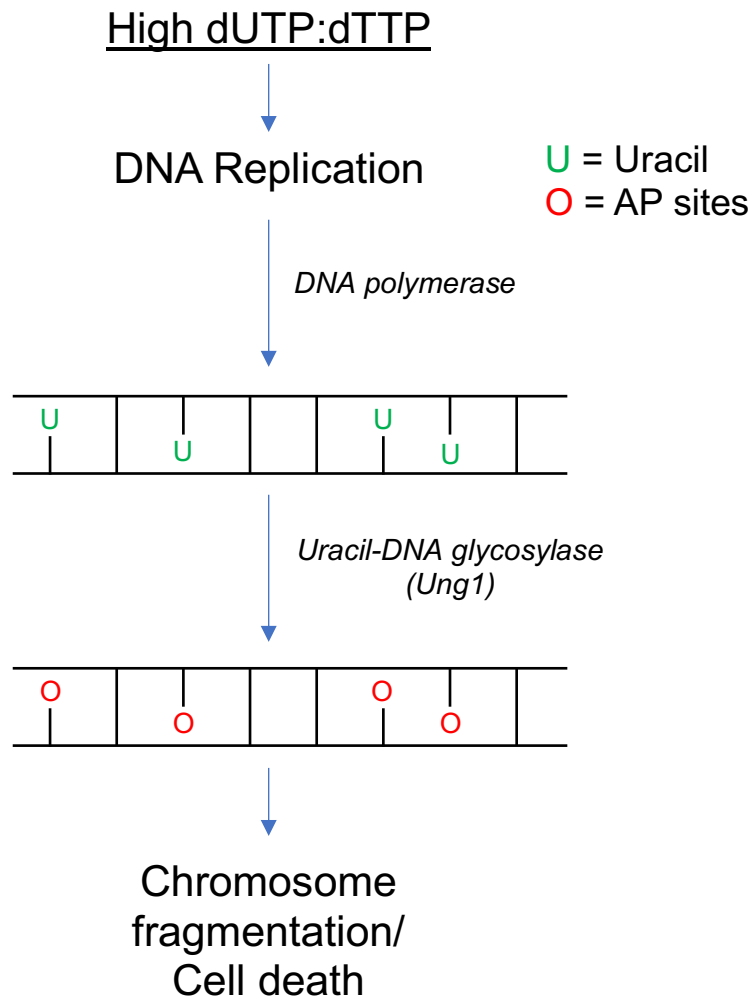


Figure 2: Uracil-mediated DNA damage.

When uracil is incorporated into DNA, this activates the enzyme uracil DNA-glycosylase, which removes uracil from DNA. This removal of uracil forms an AP site within in DNA and an accumulation of these AP sites can lead to cell death due to DNA breaks.

The mechanism to remove uracil from DNA utilizes the enzyme uracil DNA glycosylase, Ung1 in *S. cerevisiae* [22]. When uracil is incorporated, Ung1 activates and removes uracil from DNA resulting in the formation of a lesion called apurinic/aprimidinic (AP) sites or abasic sites. AP sites act to block DNA replication/repair machinery, leading to destructive outcomes, such as single-strand and double-strand breaks, resulting in fragmentation and ultimately cell death [13]. To prevent cell death, the base excision response (BER) pathway is initiated in response to specific proteins, in this case uracil DNA glycosylase. Following the removal of uracil and creation of AP sites, AP endonuclease proteins, such as APN1, incise the remaining phosphodiester bonds generating 3'-hydroxyl and 5'-deoxyribose phosphate sections. The 5'-deoxyribose phosphate end is removed by DNA deoxyribosephosphodiesterase leading to the single gaps being correctly filled in by DNA polymerase activity and further followed by DNA ligase activity to restore DNA integrity [23]. Furthermore, the mechanism as to which uracil DNA glycosylase-mediated repair is conducted varies with the initial position of uracil in the DNA relative to the replication fork [16].

In the absence of Dut1, the frequency of uracil incorporation into DNA increases due to the increase in [dUTP/dTTP] ratio, further increasing the activity of UNG1 leading to more AP sites and eventually cell death, making Dut1 an essential enzyme [24]. All dUTPase enzymes are essential enzymes in both eukaryotic and prokaryotic organisms, making this an excellent protein/pathway to target with various dUTPase inhibiting small compounds, such as in *T. brucei* [21]. In addition, sequence differences and structural differences in the dUTPase enzyme also make it a desirable protein/pathway to target. The *S. cerevisiae* and human dUTPase enzymes are both homo-trimers formed by beta-sheets and the *T. brucei* dUTPase enzyme is a homo-dimer formed by alpha helices [24, 25].

The thymidine synthesis pathway is one of the most commonly targeted pathways used to treat various types of cancer [11]. Downstream of dUTPase is the enzyme thymidylate synthase (TS), which converts dUMP to dTMP using the methyl donor 5,10-methyltetrahydrofolate (5,10-CH₂ THF). This step is essential since dTMP is required for dTTP

production, an essential precursor for DNA replication and repair. TS functions as a homodimer, containing a substrate binding site for the nucleotide dUMP and a cofactor binding pocket for 5,10-CH₂ THF. The inhibition of TS can be achieved by blocking either of the two sites. The substrate binding site can be blocked by nucleotide analogs and antifolates such as 5-fluorouracil (5-FU) and methotrexate (MTX), respectively [19, 26]. Any inhibition of TS leads to the increase in uracil level ultimately leading to thymine-less death via the UNG1 mediated repair pathway. dUTPase counteracts high levels of uracil, supplying additional pools of dUMP for TS activity to generate dTMP. dUTPase levels and activity can directly influence the very common TS-based treatment in many patients [19]. Further lowering the activity of dUTPase along with a TS-based treatment can help treat cancer patients, increasing the chances of success.

1.3 Auxin Inducible Degron System

Studying the consequences of null mutations is a very common and practical approach to study the function of a gene product *in vivo*. However, in the case of essential genes required for growth, these mutations must be conditional. Effective methods for studying essential genes utilize constructing temperature-sensitive mutants or constructing mutants with a regulatable promoter [27]. However, these two methods are problematic because temperature sensitive mutants can be laborious to generate and regulatable promoters can be leaky. A relatively new method, the auxin-inducible degron (AID), is a technique that is able to conditionally mutate a gene by degrading the target protein with no side effect in non-plant eukaryotes. Indole-3-acetic acid (IAA), or auxin, is a plant hormone responsible for regulating plant growth [28]. This compound is only found in plants, therefore when it is used in other organisms such as *S. cerevisiae*, it can be concluded that any change resulting from addition of AID is due to the presence of auxin. In budding yeast, the AID system has been successfully applied to several proteins including Dut1. The AID system utilizes the SCF E3 ubiquitin ligase complex in which auxin acts as the initiator to proteasome-mediated degradation [27, 29].

Initially, the target gene is fused with an IAA transcriptional regulator, which acts as the degron tag to induce degradation when auxin binds to it. This is followed by interaction with the F-box protein, TIR1, part of the SCF complex, which contains the recognition domain. Once properly recognized, the target protein is ubiquitylated via the E3 ubiquitin ligase, ultimately leading to its degradation by the proteasome (**Figure 3**).

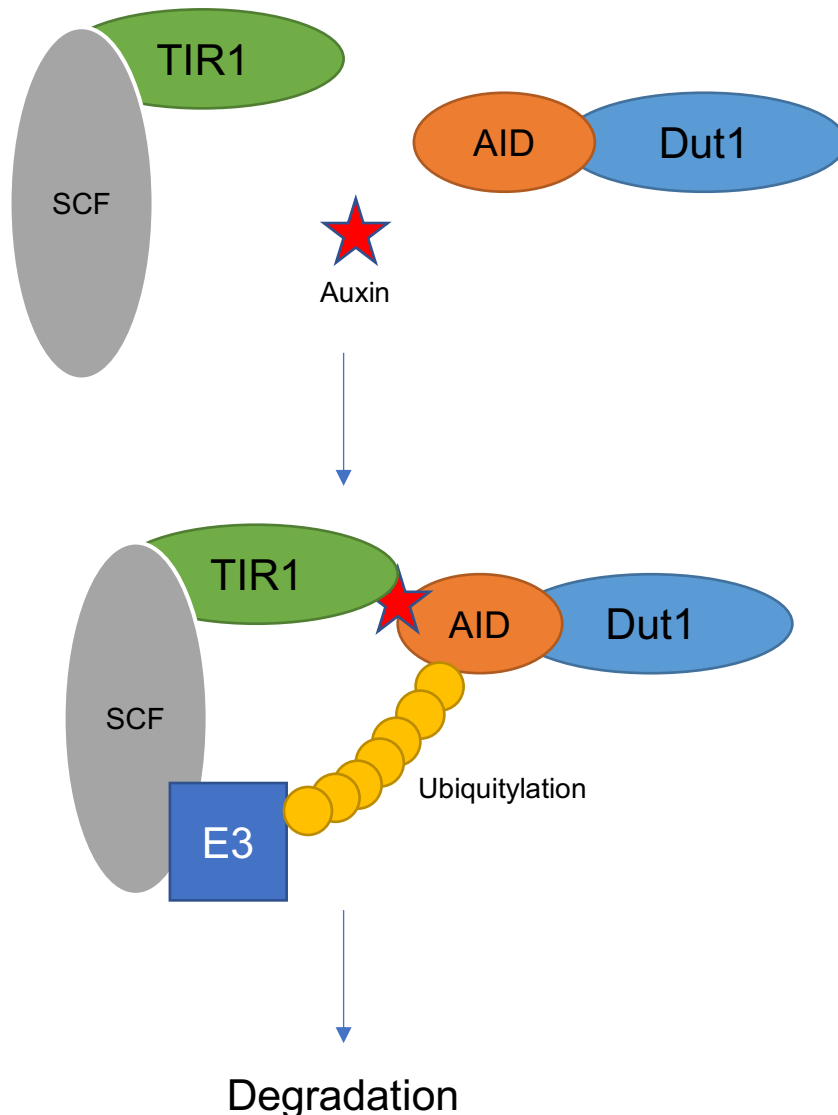


Figure 3: Auxin inducible degron system.

The addition of auxin to the culture medium among non-plant organisms, modified with degron tag and TIR1 F-box protein, allows for the rapid degradation of a protein of interest. Firstly, auxin binds to the degron tag, which then allows for the interaction with the TIR1, part of the whole SCF complex. The target protein is then ubiquitylated by E3 ubiquitin ligase, ultimately leading to its degradation by the proteasome.

Papagiannakis et al., (2017) have more recently demonstrated the effectiveness of the AID system, easily applying it to *S. cerevisiae* [29]. Utilizing the ubiquitin-mediated protein degradation system along with AID system, they were able to eliminate essential proteins of interest and create conditional mutants. The two genes they targeted were Cdc28 and Cdc14, both essential cell cycle proteins. Upon the addition of 0.1 mM auxin, they were able to show the AID system efficiently depleted the two cell-cycle proteins.

1.4 Schrödinger's Virtual Drug Screen

The conventional method for drug screening is known as high-throughput screening (HTS) [30, 31]. Specifically, for structure-based drug design, a vast number of molecules are each subjected to a reaction in the presence of a target protein, cell, etc. Depending on the assay, observational changes are then measured either by machine or manually to determine the effectiveness of the molecules being tested. This process, however, is very tedious, time consuming, and not cost effective considering that simply finding a potential candidate in a drug screen is only a starting point [32]. The advancements in technology has opened new possibilities for computer-aided drug discovery tools for a faster and more cost-efficient method, otherwise known as virtual screening [33].

Schrödinger is an emerging company in the field of biotechnology. Schrödinger offers a suite of programs that allow *in silico* simulation of molecular docking. This is achieved by using their physics-based computational platform, which allows users to evaluate a large selection of online available molecules to search for solutions through interactive and predictive modeling, molecule design, and molecular simulations. Glide is one of the programs in the Schrödinger suite, which allows for studying ligand-receptor docking [34]. For structure-based drug design, any protein structure can be uploaded to the software, if crystal structures are available. These structures can then be further prepared to simulate an active enzyme, for example adding a magnesium cofactor to a human dUTPase protein. A large database of ligands can then be run against the protein structure's active site with the software calculating multiple thermodynamic

variables. Two of these variables, docking score and binding energy, indicate how well the ligand fits into the protein's active site and how strongly the ligand binds, respectively.

Computational docking is becoming a widespread norm in the field of pharmaceuticals and biotechnology due to the programs high-throughput screening capability. This allows for a plethora of compounds to be screened for biological activity. With crystal structures available for all varieties of proteins, Schrödinger's virtual drug screening program allows the user to upload the structure to be studied, allowing for discovery at a much-accelerated rate. The uploaded protein structure can be modified to allow for a better suited structure-based drug design. Glide offers a range of screening modes, each with a varying screening speed and accuracy hits: high-throughput virtual screening (HTVS) is the fastest screening method to easily screen through millions of ligands, standard precision (SP) screens through thousands of ligands, and lastly extra precision (XP) screens through dozens to hundreds of ligands with the best accuracy scoring. Overall, Schrödinger's Glide allows for the user to achieve faster and more accurate drug design, dramatically reducing research and development costs and increasing productivity.

The combination of model organism-based genetic approach and virtual drug screening allows for a comprehensive inquiry of potential drugs and small molecules for a specific target. Structural differences in essential enzymes, such as dUTPase, in various organisms ranging from humans to trypanosomes brings forth the question: can a molecule be found that is toxic to one but not to the other? This study explores both an organism model and virtual drug screening in order to address this question. Specifically, such combinatorial approaches will be used to search for a molecule toxic to the pathogenic parasite *T. brucei* and not to the human host. Furthermore, this opens a pathway to a more cost-and time-efficient pharmacological strategy to be able to combat against various infectious diseases such as African sleeping sickness.

Chapter 2: Materials and Methods

2.1 Plasmids and Yeast Strains

The plasmids and yeast strains used for this project are listed in Table 1.

Table 1: Plasmids and Yeast Strains

Plasmids	Description	Origin
pNK14	vector pRS426	Previous study
pNK57	vector p426GAL1	Previous study
pNK258	yDUT1-3xHA; <i>BamHI</i> (5') and <i>EcoRI</i> (3')	This study
pNK259	hDUT-3xHA; <i>BamHI</i> (5') and <i>EcoRI</i> (3')	This study
pNK260	tbdUTPase-3xHA; <i>BamHI</i> (5') and <i>EcoRI</i> (3')	This study
pNK264	pGal-yDUT1-3xHA; <i>BamHI-EcoRI</i> fragment from PNK258 cloned into PNK57	This study
pNK265	pGal-hDUT-3xHA; <i>BamHI-EcoRI</i> fragment from PNK259 cloned into PNK57	This study
pNK266	pGal-tbdUTPase-3xHA; <i>BamHI-EcoRI</i> fragment from PNK260 cloned into PNK57	This study
pNK285	HO(<i>SacI</i>)-pGal-hDUT-URA3-HO(<i>MfeI</i>); flanked hDUT expression cassette with restriction sites <i>SacI</i> and <i>MfeI</i> along with HO locus sequence	This study
pNK286	HO(<i>SacI</i>)-pGal-tbdUTPase-URA3-HO(<i>MfeI</i>); flanked tbdUTPase expression cassette with restriction sites <i>SacI</i> and <i>MfeI</i> along with HO locus sequence	This study
pNK290	removed portion of tbdUTPase gene in PNK286 with restriction enzyme <i>SpeI</i>	This study
pNK296	pET22b (+)-yDUT1	Addgene; Plasmid #12667
pNK297	PNK296 transformed into BL21(DE3) competent cells	This study
pNK301	yDUT1 removed via restriction enzymes <i>NdeI</i> and <i>XhoI</i> ; ligated hDUT gene via PCR	This study
pNK303	PNK301 transformed into BL21(DE3) competent cells	This study

Table 1. Cont.		
Plasmids	Description	Origin
pNK304	yDUT1 removed via restriction enzymes <i>NdeI</i> and <i>XhoI</i> ; ligated tbdUTPase gene via PCR	This study
pNK305	PNK304 transformed into BL21(DE3) competent cells	This study
pNK306	PNK14 transformed into BL21(DE3) competent cells	This study
pNK224	pGPD2	Addgene; Plasmid #43972
Yeast Strains	Description	Origin
YNK355	- <i>LEU</i> strain	Previous study
YNK421	WT yDUT1; AFB2 gene integrated into <i>ADE2</i> locus	This study
YNK425	auxin inducible degron (AID) 6xFLAG tag added to 3' end of yDUT1 in YNK421	This study
YNK679	<i>ung1Δ</i> in YNK425	This study
YNK684	<i>URA3</i> marker; <i>ung1Δ</i> loxed-out	This study
YNK756	hDUT expression cassette integrated into HO locus of YNK425 under the control of pGal promoter with <i>URA3</i> marker	This study
YNK757	tbdUTPase expression cassette integrated into HO locus of YNK425 under the control of pGal promoter with <i>URA3</i> marker	This study
YNK760	inactive tbdUTPase expression cassette integrated into HO locus of YNK425 under the control of pGal promoter with <i>URA3</i> marker	This study
YNK766	<i>URA3</i> marker removed from YNK756	This study
YNK767	<i>URA3</i> marker removed from YNK757	This study
YNK769	<i>URA3</i> marker removed from YNK760	This study

2.2 Auxin Growth Assays

All yeast growth was performed at 30°C. To determine viable cells by the CFU assay, strains YNK421, YNK425, and YNK355 were streaked out on to agar plates containing yeast extract, peptone, and 2% dextrose (YEPD) and overnight 1 mL overnight cultures were grown in liquid YEPD as well. For YNK355, 5 mL cultures in YEPD were grown. From the overnight cultures for YNK421 and YNK425, sub-cultures were made by adding 20 μ L to 1 mL YEPD containing auxin (EtOH soluble auxin: Spectrum Chemicals; IN125 and H₂O soluble auxin: Sigma-Aldrich, I5148) at concentrations of 0, 5, 50, and 100 μ M. YNK355 cells were left growing in 30°C. After 24 hours, YNK421 and YNK425 cells were centrifuged and collected in 1.5 mL micro-centrifuge tubes, washed with 1 mL H₂O, centrifuged again and resuspended in 200 μ L of H₂O. For YNK355, 5 mL cultures were collected in 50 mL tubes and centrifuged at 3000 x g for 5 minutes and washed and resuspended in 50 mL of H₂O. YNK421 and YNK425 cells were diluted by a factor of 1×10^6 in YNK355 cell solution and plated on agar plates containing synthetic dextrose LEU dropped out (SD-LEU). THE CFU were counted after 4 days of growth and survival percentages were calculated.

For the spot growth assay, strains YNK421 and YNK425 were streaked out on YEPD and colonies on YEPD plates were used to inoculate overnight cultures in YEPD. Overnight cultures were diluted to an OD_{600nm} of 1 (approximately 5×10^7 cells/mL) and serial dilutions were made ranging from 1×10^6 to 1×10^3 cells/mL. The dilutions (5 μ L) were spotted on YEPD plates containing auxin (0, 50, 100, 500 μ M) and incubated at 30°C for 24 hrs.

2.3 Auxin Growth Curves

Growth curves were created by measuring absorbance on the BioTek Synergy plate reader at a wavelength of 600 nm. All readings were performed for 18 to 24

hours. From overnight cultures, 100 μ L was added to 5mL of media and incubated again until OD_{600nm} reached 0.6 to 0.8 and then diluted 0.1 at a final volume of 200 μ L within the 96-well plate. The following auxin [ethanol/water soluble] concentrations were used, diluted using either YEPD media or YEP-GE [YEP-GE composition with and without galactose]: 0, 5, 50, and 500 μ M. 5-fluorouracil (5-FU) was also used with auxin at the concentration of 25 μ M for specific treatment targeting the thymidine synthesis pathway.

2.4 High Throughput Virtual Screen using Schrödinger's suite.

High throughput virtual screening (HTVS) was performed using Schrödinger's Glide software. For the three-dimensional (3D) crystal structure of *T. brucei* dUTPase, the 1.47 Å resolution *T. brucei* dUTPase structure (PDB ID: 4DK2) and (PDB ID:4DL8) [25] with the "Search Space" defined as the annotated catalytic center where dUTP/dUMP binds were used. For the docking simulation of the human DUT enzyme, the annotated structures from the PDB database were used (PDB ID: IQ5U and 3ARA) [35, 36]. A custom library of 5000 compounds ("Tainer 5000") selected from the Life Chemical library for their variety, low toxicity, and drug-like properties according to the Lipinski's rules was used as the ligand library [37]. Compounds were first screened for docking into the tbdUTPase and hDUT structures' active site.

2.5 *T. brucei*/Yeast Growth Curves

The 13 molecules identified through HTVS were provided by Dr. John Tainer from MD Anderson Cancer Center. The strain YNK421 was cultured in YEPD media in a 96-well plate at a volume of 200 μ L with the starting OD_{600nm} of 0.1 with absorbance readings recorded at a wavelength of 600nm on the BioTek Synergy Plate Reader. OD_{600nm} readings were taken every 15 minutes for 20 hours. The final concentration for each of the 13 molecules was 10 μ M and methotrexate (MTX) was

used as a negative control at a final concentration of 500 μM . All samples tested contained DMSO at final concentration of 0.5% v/v.

The *T. brucei* growth assay was performed under the supervision of Dr. Kyu Joon Lee, a postdoc in the lab of Dr. Ziyin Li from McGovern Medical School, UTHealth. A stock of *T. brucei* blood-stream form (bsf) was cultured in HMI-9 medium supplemented with 10% fetal bovine serum at 37°C with 5% CO₂, in a sterile culture bottle and the medium was replenished every 2 days. To test the effect of the 13 molecules, the stock culture was diluted down to an initial target concentration of 5x10⁴ cells/mL by counting cells using a hemocytometer. Experimental cultures were made in 48-well culture plates at a final volume of 200 μL . Each of the 13 molecules were added to different wells with MTX serving as the negative control. All the compounds were at the final concentration of 10 μM and contained DMSO at a final concentration of 0.5% v/v. Cultures were grown for 4 days and 10 μL of cells were removed and counted using a hemocytometer every 24 hours.

2.6 Protein Purification

Expression vector pET22b (+)-*yDUT1* with 6X affinity His-tag was acquired from Addgene (plasmid #12667). The plasmid was purified using QIAprep Spin Miniprep Kit and transformed into BL21(DE3) competent cells for overexpression. For cloning of hDUT and tbdUTPase sequences, pET22b (+)-*yDUT1* was first cut with *NdeI* and *XhoI* to remove the *yDUT1* sequence. The hDUT sequence was PCR amplified using F primer: TAAGCACATATGCCATGTAGTGAAGAGAC and R primer: TGCTTACTCGAGATTTTTGCCGGTACTACC. The tbdUTPase sequence was PCR amplified using F Primer: TAAGCACATATGAAAACGCGCGTCGTG and R primer: TGCTTACTCGAGACTCTTCAACCAGTGACC. The amplified PCR products were ligated to *NdeI/XhoI* cut pET22b (+)-*yDUT1*. Both ligations were confirmed by sequencing (Eurofins Scientific) using T7 and T7term primers, followed by

transformation into BL21(DE3) cells for overexpression. For a negative control, empty vector pRS426 was transformed into BL21(DE3) competent cells.

Protein purification was performed as described previously in Dabrowski and Ahring (2003), [38], with some modification as described below. All four BL21(DE3) cell types were grown overnight in 5 mL of LB-ampicillin. Subcultures were then started in 500 mL of LB-Ampicillin-0.1% Glucose media and growth was monitored until an OD_{600nm} of 0.3-0.5 was reached. IPTG was added at a final concentration of 0.5 mM and cultures were grown for an additional 4 hours. The cells were harvested by centrifugation at 4,000 x g for 10 minutes at 4°C and the supernatant was removed, and the cells were stored in -80°C. Overexpression was confirmed by collecting cells before and after IPTG induction and Western immunoblotting was performed on the whole cell extracts. Thawed frozen cells were resuspended in 20 mL of Buffer A (20 mM Tris-HCl pH 8.0, 500 mM NaCl, 5 mM Imidazole, 0.1% Triton X-100, Protease Inhibitor Cocktail II, EDTA Free (10X)) and then sonicated for a total of 12 minutes (2 seconds on/off). They were then centrifuged at 18,000 x g for 20 minutes at 4°C and lysate was collected along with a small 50µL aliquot and stored in 4°C. 2 mL of HisPur Ni-NTA Resin (Thermo Scientific, Prod # 88221) was added to the cell lysate and mixed overnight at 4°C. The column for protein purification was set up and lysates containing Ni-NTA resin was added to the column and the flow through was collected. Small 50 µL aliquots were collected from the flow through as well. The Ni-NTA resin was washed with 30 mL of Buffer A-50 (Buffer A with 50 mM imidazole) and 30 mL of Buffer A-80 (Buffer A with 80 mM imidazole) and lastly eluted with 10 mL of Elution Buffer (Buffer A with 500 mM imidazole). 50 µL aliquots also collected after the two wash steps and the elution was collected in 1 mL aliquots. The purity was checked by electrophoresis of all collected aliquots and elution through a Novex WedgeWell 4-20% Tris-Glycine Gel (Thermo Scientific) and

staining with EZ-RUN Protein Gel Staining Solution (Fisher Scientific, Prod # BP3620-1). Elution tubes 7-10 were combined and desalted with an Amicon Ultra-4 10K Centrifugal Filter (Millipore, Prod # UFC801008). Then the purified protein was resuspended in Storage Buffer (20 mM Tris-HCl pH 8.0, 50 mM KCl, 50% Glycerol, 0.5 mM PMSF) and stored at -80°C until it was ready for use. Protein quantification was performed via QuantiChrom Protein Assay Kit (BioAssay Systems, Prod # QCPR-500) with BSA as a standard.

2.7 Western Immunoblotting

dUTPase protein levels were visualized by Western immunoblot of the crude cell lysates. Cells were first adjusted to an appropriate OD_{600nm} and the cell pellets were resuspended in 100 µL of dH₂O and 100 µL of 0.2 M NaOH and incubated at room temperature for 5 minutes. Cells were centrifuged and resuspended in 50 µL of SDS sample buffer and heated for 5 minutes at 95°C. All samples and the protein ladder (Xpert 2 Prestained Protein Marker) were loaded in volumes of 10 µL in Novex WedgeWell 10% Tris-Glycine Gel and initially run at 90 V for 10 minutes followed by 150 V for 30 minutes in SDS Running Buffer. The proteins were transferred from the gels to PVDF Membrane using Semi-Dry Transfer. All membranes were blocked with 5% milk in 1X TBS + 0.1% Tween overnight at 4°C. The primary and secondary antibody treatments were also performed overnight at 4°C. Anti-Flag antibody treatment did not require a secondary antibody treatment, since it was conjugated with horseradish peroxidase (HRP). Anti-Nsr1 and Anti-His antibody treatments required a secondary antibody treatment of Anti-Mouse-HRP. For blot visualization, blots were treated with West-Q Femto ECL Solution for 3 minutes and then imaged on Bio-Rad ChemiDoc MP Imaging System.

2.8 Pyrophosphate-based Enzymatic Activity

Enzymatic activity was measured using the PiPer Pyrophosphate Assay Kit's "Measuring Enzymatic Activity" protocol (Thermo Scientific, Prod # P22062). For the three purified proteins, yDut1, hDUT, tbdUTPase, and our vector control, 500 ng was used for each purification and dUTP was used at a concentration of 0.5 mM. Fluorescence was measured using the BioTek Synergy Plate Reader at excitation and emission wavelengths of 575/15 and 620/15 nm respectively. Readings were recorded every one and a half minutes for one hour at a temperature of 37°C.

2.9 PCR-based Enzymatic Activity

A mix of individual dATP, dCTP, and dGTP and either dTTP or dUTP were utilized for PCR reactions. 5 µL of 5 mM dUTP or dTTP were incubated for 24 hours at 37°C with 5 µL of each purified protein; yDut1, hDUT, tbdUTPase, and vector control in 10 µL of reaction buffer (100 mM Tris-HCl pH 7.5, 20 mM MgCl₂, 20 mM DTT, and 0.2 mg/mL BSA). The reactions were stopped by freezing and storing samples at -20°C. PCR reactions were set up utilizing Taq DNA Polymerase (Fisher Scientific, Prod # FB-5000-50) and MyTaq DNA Polymerase (Bioline, Prod # BIO-21105) using the reaction concentrations according to the manufacturer's recommendations. In place of a dNTP mix, dUTP or dTTP treated with yDut1, hDUT, tbdUTPase, or the vector control was added to the mix of dATP, dCTP, dGTP at 2 mM each. PCR cycles were set as follows: 1 cycle of 95°C for 5 minutes, 35 cycles of 95°C for 30 seconds, 60°C for 30 seconds, and 72°C for 1 minute, 1 cycle of 72°C for 7 minutes, and hold at 4°C. PCR products were separated on 1% agarose gels and visualized using the Bio-Rad ChemiDoc MP Imaging System.

Chapter 3: Results

3.1 Auxin growth assay/curves showing growth inhibition in the presence of auxin

The overall objective of this project was to discover a small molecule that binds and inhibits the function of *T. brucei* dUTPase but has no effect on human DUT or yeast Dut1. Since the dUTPase enzyme is essential for cell viability in *T. brucei* as well as in humans, a small molecule with such discriminatory properties will have a great potential as an anti-parasitic drug to combat African sleeping sickness. To accomplish this goal, I proposed: 1) to determine if the dUTPase proteins from human and *T. brucei* can functionally complement the absence of Dut1 in *S. cerevisiae*, and 2) to discover and characterize a list of possible small molecules that inhibit the function of *T. brucei* dUTPase.

As described in Chapter 1, the dUTPase enzyme is essential in all organisms, making it an excellent target for a small molecule to bind to and inhibit its function, ultimately killing its host organism. Being able to use yeast a model system to express human and *T. brucei* dUTPase genes would allow us to screen for a drug or small molecule and achieve our overall objective. I hypothesize that this is possible due to the differences in protein structure of *T. brucei* and human/yeast dUTPases **(Figure 4)**.

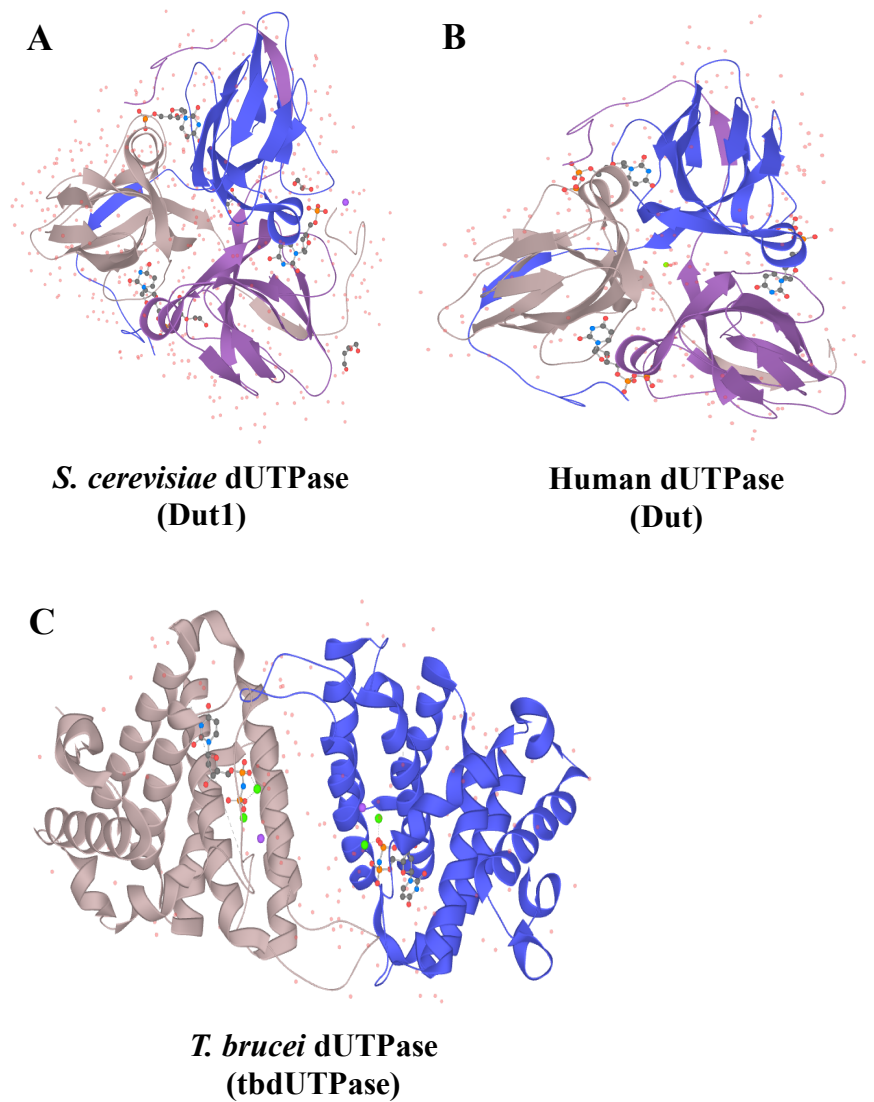


Figure 4: dUTPase crystal structures.

(A)yDut1 [24], (B)hDUT [35], and (C)tbdUTPase [25] 3D crystal structures. yDut1 and hDUT are homo-trimers formed by beta-sheets, whereas tbdUTPase is a homo-dimer formed by alpha-helices.

Furthermore, because dUTPase is essential, conventional null mutation methods are not feasible to study this enzyme. Here, I used in the budding yeast, *S. cerevisiae*, a conditional knockdown method known as the auxin inducible degron (AID) system. The strain YNK425, which contains the *DUT1* gene with C-terminally located AID-tag (*ydut1-AID*), was created by a previous lab member, Dr. Norah Owiti. This allows us to utilize the AID system to knockdown the dUTPase enzyme in the presence of auxin. The effectiveness of the AID system was shown in numerous ways. First, a simple CFU assay was performed to show that in the presence of auxin at a concentration of 5 and 50 μM , the survival rate for YNK425 is reduced in comparison to two isolates of YNK421 (*WT yDUT1*) (**Table 2**). Survival rates were calculated relative to the cultures grown without auxin. Overall, auxin does not inhibit the growth of YNK421, but does indeed inhibit the growth of YNK425. Cell growth was maximally inhibited when cells are grown in the presence of 50 μM auxin. Although there are some cultures/replicates that had a high survival rate for YNK425, similar to when treated without auxin, the overall trend remained the same where the strain's survival decreased in the presence of auxin. These replicates with outlying results may be the result of suppressor mutations arising during overnight growth.

Table 2: CFU Assay showing survival rates of WT yDUT1 and ydut1-AID.

Auxin Concentration	Strain	Plate 1 Count	Plate 2 Count	Total Count	Survival Rate
5 μ M	WT DUT1	145	186	331	98%
	WT DUT1	212	151	363	86%
	WT DUT1	185	174	359	114%
	WT DUT1	209	177	386	97%
	WT DUT1	140	162	302	78%
	WT DUT1	166	142	308	87%
	ydut1-AID	188	179	367	120%
	ydut1-AID	12	9	21	58%
	ydut1-AID	5	15	20	91%
	ydut1-AID	42	38	80	29%
	ydut1-AID	50	47	97	41%
	ydut1-AID	41	40	81	30%
50 μ M	WT DUT1	161	158	319	95%
	WT DUT1	198	195	393	93%
	WT DUT1	137	179	316	100%
	WT DUT1	162	175	337	84%
	WT DUT1	165	214	379	98%
	WT DUT1	184	201	385	108%
	ydut1-AID	152	152	304	99%
	ydut1-AID	2	2	4	11%
	ydut1-AID	1	5	6	27%
	ydut1-AID	9	15	24	9%
	ydut1-AID	38	46	84	35%
	ydut1-AID	14	21	35	13%

To further show that the AID system is functioning properly, the strain YNK684 (*ydut1-AID ung1Δ*) was also grown in the presence and absence of auxin. In YNK684 the, *UNG1* gene encoding the uracil DNA glycosylase is deleted, thus the uracil in the DNA is no longer removed and AP sites are not generated. Therefore, it is expected that in YNK684, the increase in the level of uracil in DNA when Dut1 is degraded by auxin would have less effect. YNK684 was grown and treated with 50 μM or 100 μM auxin and subjected to the CFU assay (**Table 3**). Survival rates were calculated relative to the cultures grown without auxin. As can be seen in the table, all replicates for both isolates for YNK684 show a high survival rate in the presence of both 50 μM and 100 μM auxin, whereas YNK425 shows a low survival rate for both auxin concentrations. For both strains there are replicates that are outliers and do not follow the expected trend for their respective strains, which again is most likely due to suppressor mutations. However, for YNK684, where a 56.00% survival rate is seen for YNK684 in 100 μM auxin, the outliers may be due to technical errors when preparing cultures resulting in low colonies formed. The dashes in the table represent no colonies were grown in the plate. Therefore, in the cases in which one of the plates did not have any colonies, the number of colonies grown on the other plate was doubled to calculate the survival rate.

Table 3: Auxin CFU Assay showing survival rates for YNK425 and YNK684.

Auxin Concentration	Strain	Plate 1 Count	Plate 2 Count	Total Count	Survival Rate
50 uM Auxin	ydut1-AID	-	7	14	6.73%
	ydut1-AID	15	20	35	16.36%
	ydut1-AID	9	5	14	5.17%
	ydut1-AID	24	24	48	21.05%
	ydut1-AID	14	6	20	8.20%
	ydut1-AID	23	23	46	22.01%
	ydut1-AID	9	9	18	7.76%
	ydut1-AID	106	89	195	87.05%
	ydut1-AID	21	5	26	13.27%
	ydut1-AID	22	17	39	18.57%
	ydut1-AID ung1Δ	76	108	184	88.46%
	ydut1-AID ung1Δ	125	68	193	96.50%
	ydut1-AID ung1Δ	108	109	217	93.94%
	ydut1-AID ung1Δ	113	101	214	91.45%
	ydut1-AID ung1Δ	154	112	266	105.14%
	ydut1-AID ung1Δ	118	118	236	112.38%
	ydut1-AID ung1Δ	141	107	248	124.00%
	ydut1-AID ung1Δ	99	96	195	100.00%
	ydut1-AID ung1Δ	154	117	271	115.81%
	ydut1-AID ung1Δ	106	88	194	79.51%
100 uM Auxin	ydut1-AID	5	11	16	7.69%
	ydut1-AID	9	22	31	14.49%
	ydut1-AID	7	15	22	8.12%
	ydut1-AID	18	21	39	17.11%
	ydut1-AID	16	9	25	10.25%
	ydut1-AID	13	18	31	14.83%
	ydut1-AID	18	14	32	13.79%
	ydut1-AID	115	87	202	90.18%
	ydut1-AID	11	9	20	10.20%
	ydut1-AID	23	17	40	19.05%
	ydut1-AID ung1Δ	89	114	203	97.60%
	ydut1-AID ung1Δ	95	98	193	96.50%
	ydut1-AID ung1Δ	88	81	169	73.16%
	ydut1-AID ung1Δ	106	84	190	81.20%
	ydut1-AID ung1Δ	94	112	206	81.42%
	ydut1-AID ung1Δ	-	102	204	97.14%
	ydut1-AID ung1Δ	56	56	112	56.00%
	ydut1-AID ung1Δ	111	74	185	94.87%
	ydut1-AID ung1Δ	120	108	228	97.44%
	ydut1-AID ung1Δ	-	123	246	100.82%

“-“ represent no colonies were grown

The CFU assay shows that the AID system in the strain YNK425 is functional and effective in conditionally knocking down the essential enzyme Dut1 in *S. cerevisiae*. However, due to inconsistencies with the CFU assay in terms of colony counting and survival rates, the effectiveness of the AID system in YNK425 was also examined using the spot growth assay (**Figure 5**) and growth curves determined by using a plate reader (**Figure 6**). In Figure 5, four different auxin concentrations were tested on YEPD plates; 0, 50, 100, and 500 μM . The growth of *ydut1-AID*-containing YNK425 is significantly inhibited as the auxin concentration increases due to the presence of the AID system causing the degradation of *yDUT1*. Conversely, the wild-type *yDUT1*-containing strain YNK421 shows no reduction in growth under any of the auxin concentrations. The smeared culture on the 0 μM auxin plate for YNK425 was due to a pipetting error. Figure 6 also includes the strain YNK679 (*ydut1-AID-ung1 Δ*), which is expected to show no signs of growth inhibition, because although grown in the presence of auxin, AP sites do not form due to the absence of *UNG1*. The growth curves shown in Figure 6 consist of YNK421, YNK425, and YNK679 incubated in YEPD and at three different auxin concentrations (0, 50, and 500 μM). When YNK425 is treated with 50 μM or 500 μM auxin, there is a significant inhibition in the growth rate in comparison to when YNK425 is not treated with auxin. In addition, YNK421 and YNK679 grow to a saturation point as expected with and without auxin. It can be noted that YNK425 does not grow as well as the other two strains even in absence of auxin. This may be because the AID-tag may slightly interfere with Dut1 function.

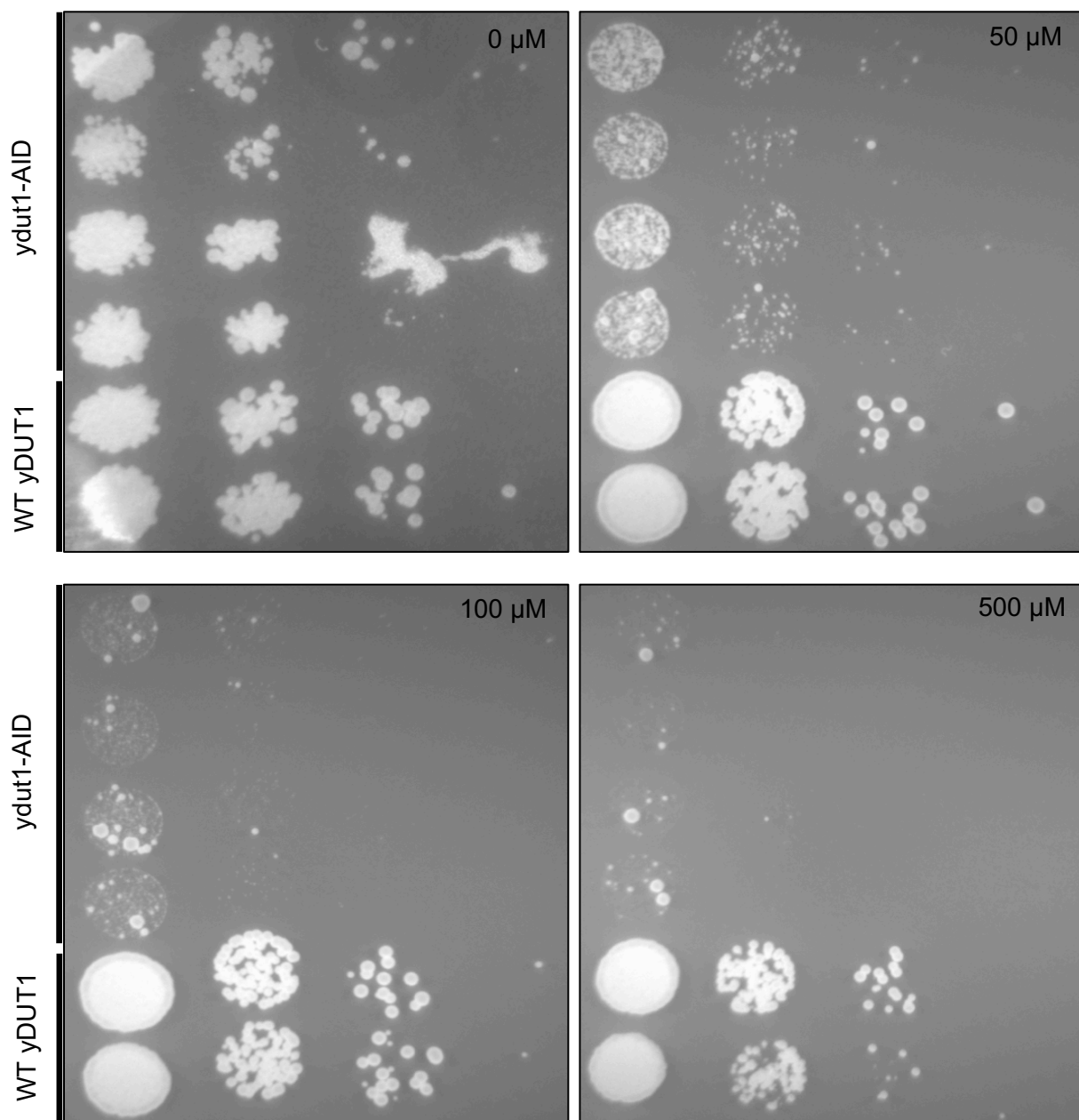


Figure 5: Spot growth assay with and without auxin.

Cultures for strains *ydut1-AID* and *WT yDUT1* were serially diluted and spotted on YEPD plates containing 0 μM (top left), 50 μM (top right), 100 μM (bottom left), and 500 μM (bottom right) auxin.

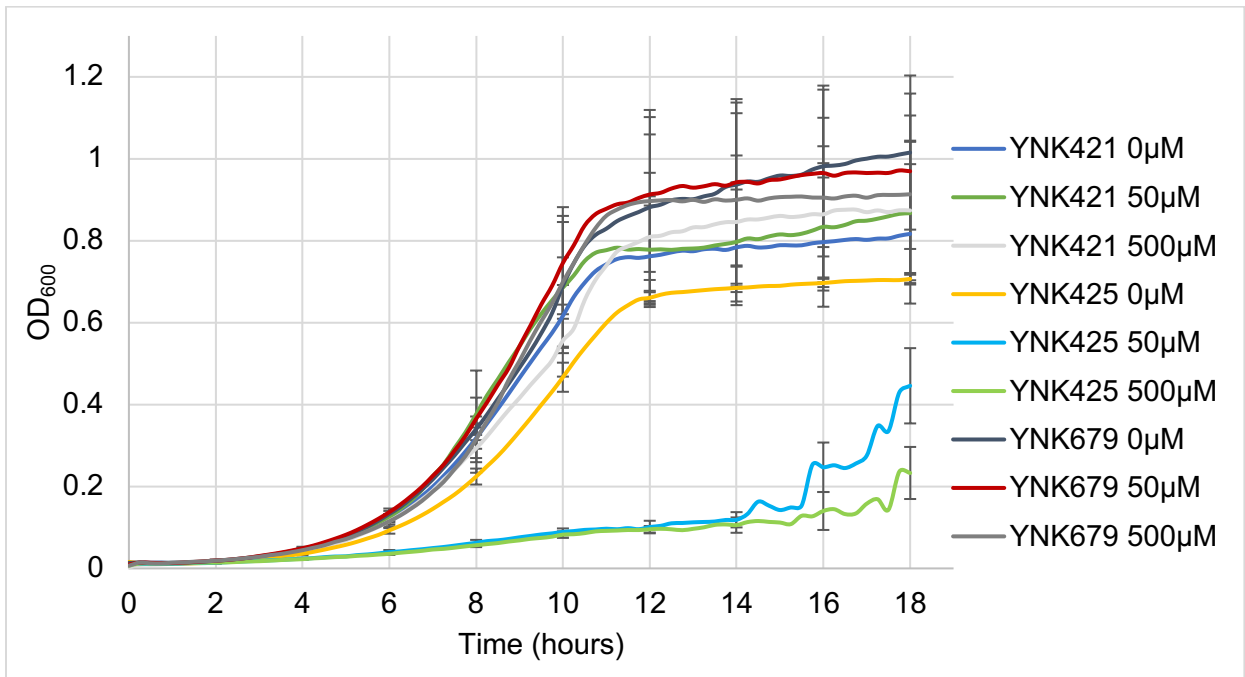


Figure 6: Growth curves showing effectiveness of AID system.

OD_{600nm} measurements over indicated time in hours for YNK421, YNK425, and YNK679 in the presence of 0, 50, and 500 μM auxin in YEPD media utilizing BioTek plate reader. N = 8 for each strain and auxin condition.

After observing growth inhibition of YNK425 in the presence of auxin, we next wanted to confirm the AID system's specificity and visually demonstrate the auxin-dependent degradation of the Dut1 protein. Since the Dut1 protein is 3X-Flag tagged in addition to the AID tag in YNK425, visualization of its degradation in the presence of auxin is made possible using Western immunoblotting with anti-Flag antibody. Subcultures of YNK425 were started and initially grown for 4 hours before adding auxin to have an equal Dut1 expression level for cultures treated with and without 50 μ M auxin. Growth measurements at OD_{600nm} were also recorded to ensure the same number of cells were loaded onto the gels for each timepoint to track the degradation of Dut1 in the strain YNK425 (**Figure 7**). Cells were collected and extracts were prepared at 0, 2, and 6 hour timepoints. It can be clearly seen that after 2 hrs of treatment with 50 μ M auxin, the amount of Dut1 protein is greatly reduced, but recovers at 6 hours. Without any auxin, the expression of Dut1 does not change significantly over the time examined.

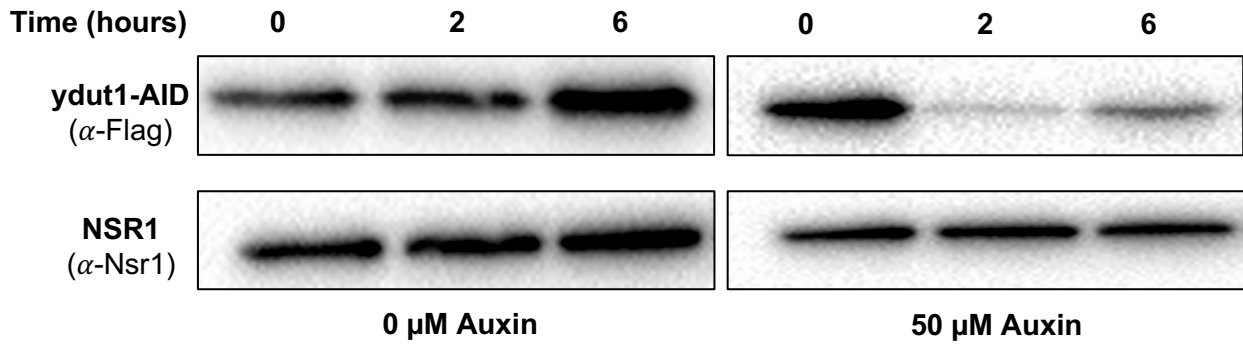


Figure 7: Degradation of Dut1 in YNK425.

Cell extracts were collected at 0, 2, and 6 hour timepoints to create a western blot showing the degradation of Dut1 when treated without auxin (left) or with 50 μ M auxin (right). 3X-Flag tagged ydut1-AID was detected using anti-Flag antibody. Anti-Nsr1 antibody was used as a loading control.

The auxin CFU assay, spot growth assay, and growth curves that have been presented all prove that the AID system is indeed functional in the strain YNK425 and effectively degrades the dUTPase protein in the thymidine synthesis pathway. Since this pathway is heavily targeted by well-studied molecules such as 5-FU (**Figure 8A**), we then sought to see how YNK425 behaves in the presence of auxin as well as 5-FU. This experiment was conducted to determine whether the combination of 5-FU and auxin would have a synergistic effect on the cell growth in YNK425 due to an increase in [dUTP/dTTP] (**Figure 8B**). This was tested with another growth curve analysis using a plate reader. The auxin concentrations used for this were 0, 5, and 500 μM along with and without 25 μM 5-FU. Initially, 10 μM of 5-FU was used, but the difference in cell growth was less than significant (data not shown). It can be seen that when 25 μM 5-FU is added to 0 μM and 5 μM auxin, you do see an additive effect in cell growth inhibition is observed. However, at 500 μM auxin there is less cell growth with 5-FU added, but the difference is too small to make any significant conclusion. Overall, it can be stated that auxin in combination with 5-FU does help with inhibiting cell growth in the strain YNK425.

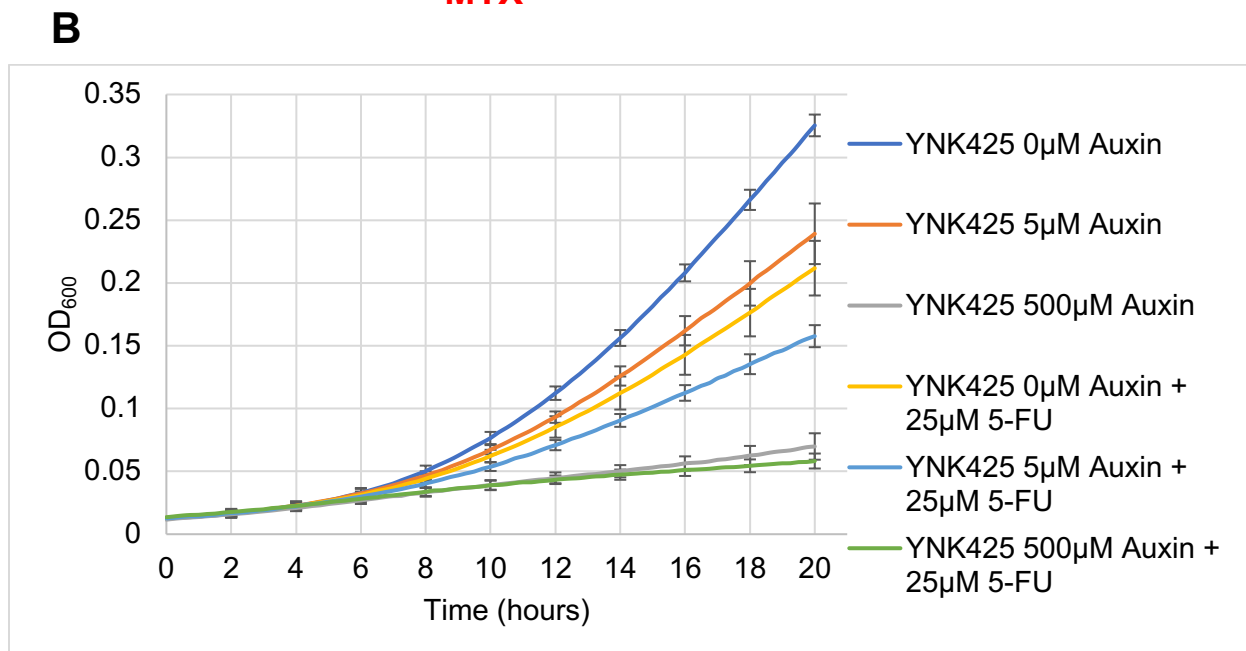
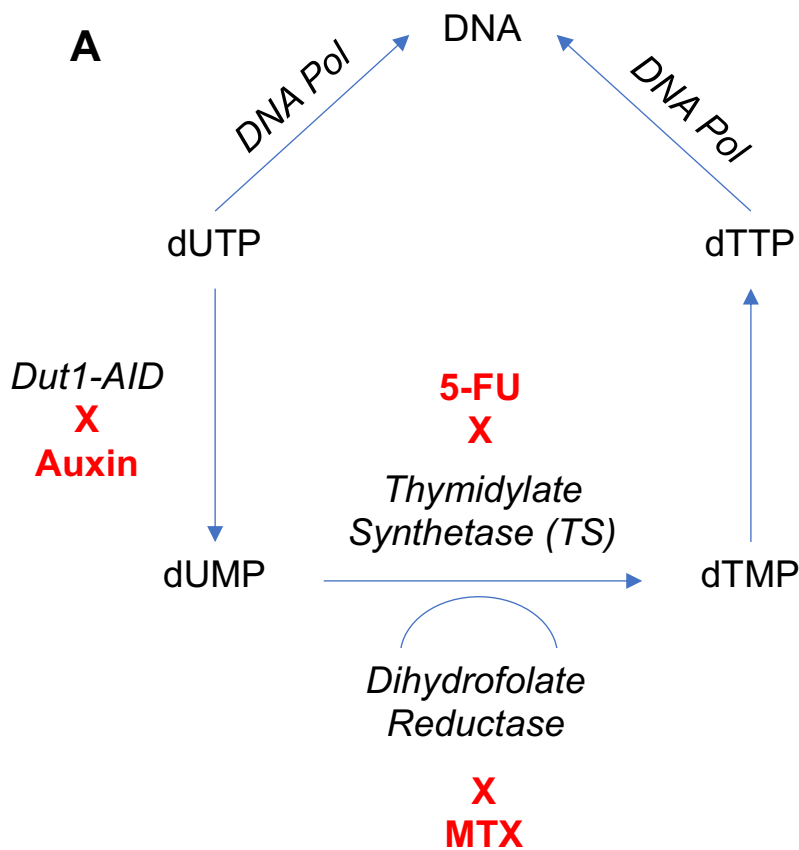


Figure 8: dTTP synthesis pathway and the targets of auxin, 5-FU, and MTX.

(A) 5-FU and MTX are well known drugs that target thymidylate synthetase and dihydrofolate reductase, respectively, in the thymidine synthesis pathway. **(B)** Growth curve of YNK425 with and without auxin and 25 μM 5-FU, grown in YEP-GE 2% galactose media.

3.2 Expression of human and *T. brucei* dUTPase in yeast

With the overall objective being to discover a small molecule that inhibits tbdUTPase, next I tested if dUTPase genes from yeast, human, and *T. brucei* on plasmids under a galactose inducible promoter could be transformed into YNK425 and compliment the low level of dUTPase when the native Dut1 protein is conditionally knocked down in the presence of auxin. **Table 4** below shows the sequences used for yeast, human, and *T. brucei* dUTPase genes. The sequences also contain a HA tag which allowed for their expression to be confirmed. This was performed by a previous graduate student, Dr. Norah Owiti. The plasmid structure containing dUTPase genes is shown in **Figure 9**.

Table 4: dUTPase gene sequences for yeast, human, and *T. brucei*

yDUT1 (PNK264)	ATGACTGCTACTAGCGACAAAGTACTAAAGATTCAATTGCGCTCAGCAAGCGC TACTGTACCTACCAAAGTTCTGCCACTGCCGCGGGATACGACATTTATGCAT CTCAGGATATTACCATTCCGGCTATGGGTCAAGGTATGGTTTCCACCGACATAT CGTTCACCGTACCTGTTGGTACCTACGGTCTGATTGCGCCAAGGTCAGGCCCTG GCAGTGAAAAACGGTATCCAAACCGGTGCTGGTGTGTCGACAGAGATTACAC CGGTGAAGTTAAAGTAGTTTTATTCAATCATTACAGAGGGATTTCCGCGATCAA AAAAGGTGATCGCGTAGCCCAATTGATTCTGGAAAAAATTGTCGATGATGCC AGATCGTTGTTGTAGACTCTCTGGAAGAAAGTGCAAGAGGGGCCGGTGGCTTT GGTAGCACTGGTAAC
hDUT (PNK265)	ATGCCATGTAGTGAAGAGACTCCGGCTATTTCTCCGAGTAAGAGAGCGAGGCC CGCTGAGGTGGGTGGAATGCAACTACGTTTCGCCAGATTGAGTGAACATGCAA CGGCCCTACTAGAGGTAGTGCCAGGGCTGCCGGGTATGACCTGTACTCAGC GTATGATTATACGATCCCCCCCATTGAAAAAGCTGTTGTAAAGACCGATTTCA AATTGCCCTGCCCTCTGCTGTACGGAAGGGTAGCTCCAGAAAGTGGGCTT GCCGCTAAGCACTTCATAGATGTGGGAGCAGGAGTAATTGATGAGGATTATCG TGGCAACGTGGGAGTAGTCTTGTTTAACTTTGGTAAGGAGAAATTCGAGGTGA AAAAAGGGATAGAATAGCGCAGTTGATTTGTGAAAGAATCTTCTATCCTGAAA TCGAGGAAGTCCAGGCCCTTGACGACACGGAGAGGGGTAGCGGTGGATTTGG TAGTACCGGCAAAAAT
tbdUTPase (PNK266)	ATGAAAAACGCGCGTCTGTGTCCCTAAGCCCCCTAATTTTAAGGAGCCTTGC CGAGTTGCAAGATGGACTTAATACCGTGGTAGATAAAAACTGGAGACAGTTGA GGAGACCAGGTGACTGGTCCTTGGCCATCACTATGGAGGCAGCAGAATTGCTT GACAGCTATCCGTGGAAGTGGTGGAAAAATGTAAAGGCGCAACCCGATTTGCA GAACGTAAAGATTGAGCTGACCGACATCCTTCACTTTTCTCTTAGCGGGGCAAT GCAGGTCTCTGATGAGAACAGTGGAGCCGTGCACAAGGCAGAGGCTGGCTCC AATGGGGAGTCAGGAAAACATTGGTGTATTTTCGACCAGCCAAGAGCGTTGCC CGCCGCGGGCGGGCGGGAATATGTCGCGTGCCTTGAACACCTGGCTCATCA TTGAGCGCACCAAGTCAGTGCAGACGAGTGCAGCCTGGCGGACTTCATGTTCTT CCCGCTGAGTGATACTAATAATGCACTAGCCTCTTTCCAAAATATAATCAGACT GGCCTCATTACAAAGATTTCACTAGTAACATCTGCTGTTATTGCAGCGGCGGA TGACATTGGGTTTAATCTGGTGCCTACTATGTAGCTAAACATACGTTGAACGG CATTTCGTCAGATGAAGGGCTATAAGGATGGAACCTACGTCAAGGTACAAAAAG GTGTTGAAGATAATGAGTTACTTCACGGGTGCATTTCTCCATTTTCCCTTGACG ATGTCACGAATGAAGGGAATTACAAGACTAAGTGGGACGATATTATGCACCGT GTTTATGACGCGTTTGGGACGCCCAAGGAGGAAAGACTAAATATAGGTCACTG GTTGAAGAGT

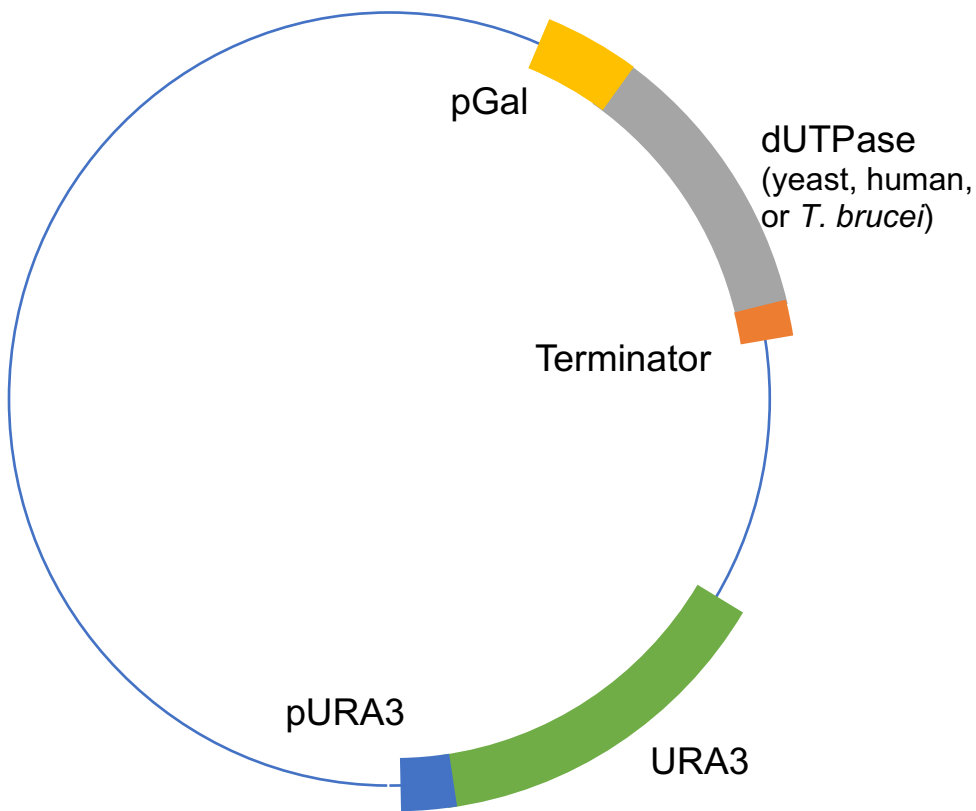


Figure 9: General structure of plasmids containing yeast, human, and *T. brucei* dUTPase genes.

The dUTPase genes are under the control of a galactose inducible promoter and also contain a 3X-HA tag. The inducible promoter allows for controlling its expression and the HA tag allows for monitoring said expression. The plasmids also contain a URA3 marker for selectivity on SD-URA plates following LiAc transformation.

Plasmids containing vector control, yDUT1, hDUT, and tbdUTPase were purified and then transformed into YNK425 using standard lithium acetate (LiAc) yeast transformation protocol and selected for on SD-URA plates. Appropriate colonies were selected to test for the functional complementation of yDUT1, hDUT, and tbdUTPase using two assays: CFU assay and growth curves (**Table 5 and Figure 10**). Survival rates for Table 5 were calculated relative to the cultures grown without auxin.

Table 5: CFU assay of YNK425 transformed with vector, yDUT1, hDUT, and tbdUTPase plasmids.

CFU Assay (50 μM Auxin)				
Plasmid	Vector	yDUT1	hDUT	tbdUTPase
Survival	96%	85%	71%	69%

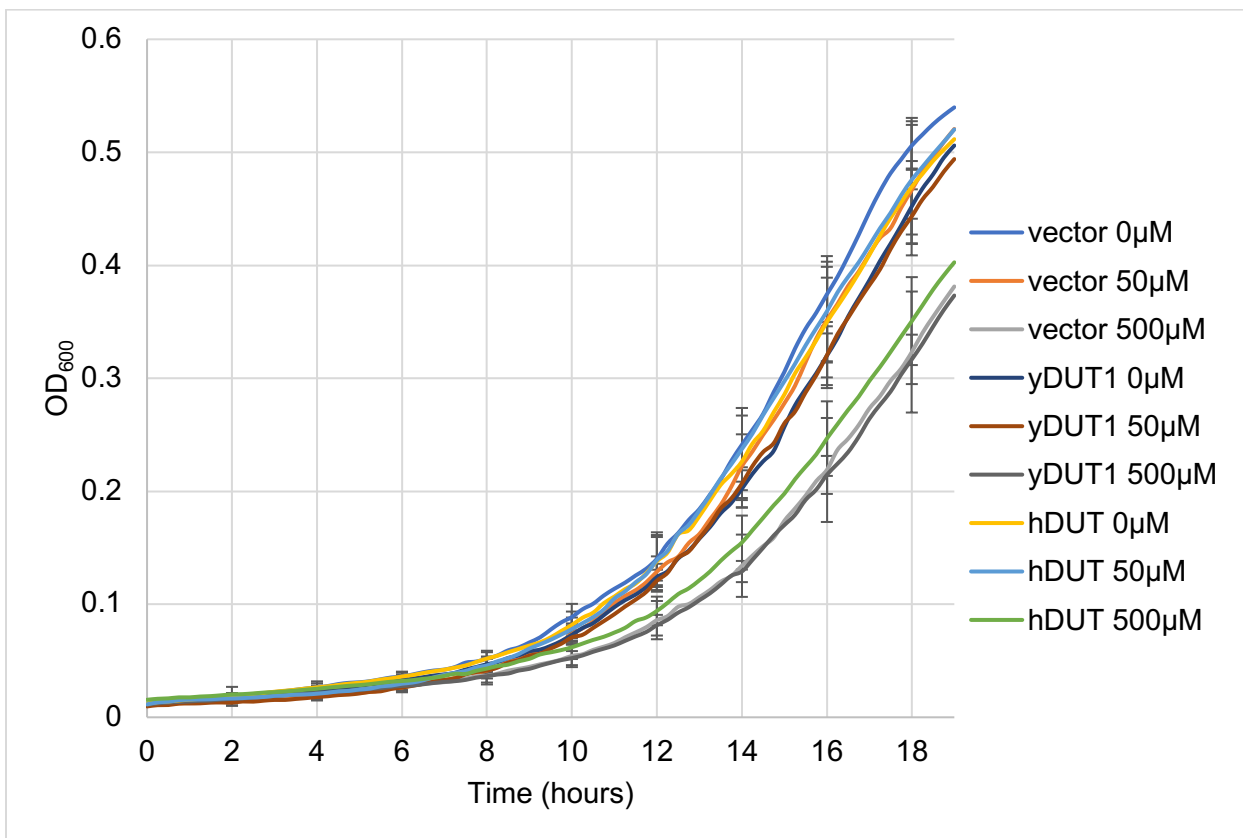


Figure 10: Assay testing functional complementation following yeast transformation.

Growth curve of YNK425 transformed with vector, yDUT1, or hDUT plasmids grown in SD-URA 2% galactose/raffinose media with the addition of indicated concentration of auxin (0, 50, or 500 μM).

In Table 5, yDUT1, hDUT, and tbdUTPase plasmids transformed into YNK425 in the presence of auxin are expected to have significantly higher survival rates than the vector. However, the vector plasmid transformation shows the highest survival rate when the transformants are grown in the presence of 50 μ M auxin. The data shown in Table 5 is just one of the several trials that was performed. All had the same results where the cell survival of vector transformed YNK425 was not different or was better from the other three plasmids in presence of 50 μ M auxin. Due to inconsistencies that have been observed before with the CFU assay, the transformants were tested by generating growth curves using the plate reader. Figure 10 does not have data for tbdUTPase transformants in YNK425 because of the low number of colonies formed, which was not sufficient enough to create a growth curve. Therefore, I proceeded to use only vector, yDUT1, and hDUT transformants. All cultures were initially diluted to 0.1 OD_{600nm} to start with an equal number of cells. The SD-URA 2% galactose/raffinose medium was used which resulted in a low max OD_{600nm} of approximately 0.5. The growth of transformed cells was measured in three different auxin concentrations, 0, 50, and 500 μ M. In the presence of 50 or 500 μ M auxin, cells transformed with the vector control was expected to show a significant inhibition in growth rate because of the degradation on the native Dut1 with no other dUTPase to complement its loss. However, we observed that the vector control-transformed cells at both concentrations of auxin grows almost similar to vector control with no auxin as well as the yDUT1- or hDUT-transformed cells. Both the CFU assay and growth curve analysis were performed several times giving the same result. To combat this, a few changes were attempted including using a commercially available SC-URA amino acid mix (Sunrise Science Products; Prod 1306-030), using YEP-GE 2% galactose media instead of using SD-URA 2% galactose/raffinose media, and instead of an ethanol-soluble auxin, using a water-soluble auxin. All these changes resulted in the same outcome with

complementation not being able to be proven, due to no cell growth inhibition observed in cells transformed with the vector control (data not shown).

In an alternative approach to the plasmid transformation, we moved on to integrating the dUTPase protein-expressing cassette into the yeast genome. A proper locus to integrate the dUTPase genes into the yeast genome would be where normal yeast functions would not be disrupted by the integration. In Dr. Kim's lab, all of the yeast strains being used are MAT α haploid strains, therefore genes involved in mating functions are considered to be neutral or non-functional genes. One such gene is the *HO* gene, encoding an endonuclease necessary for mating type switching from MAT α to MAT α and vice versa [39]. In order to incorporate hDUT and tbdUTPase into the *HO* gene, the previously used plasmids consisting of hDUT and tbdUTPase were modified to include sequences from the *HO* gene upstream and downstream of pGal and URA3 marker along with *NotI* restriction sites to cut out the desired region of the modified plasmid. The modified fragments were transformed into the strain YNK425 and were integrated into the yeast genome via homologous recombination.

The hDUT and tbdUTPase genes incorporated into the yeast genome are HA tagged. Therefore, I first checked to see if these proteins were properly expressed in YNK425 by Western blotting with anti-HA antibody (**Figure 11**). Both hDUT and tbdUTPase proteins are well expressed when grown in YEP-GE 2% galactose media in comparison to just YEP-GE media, in which they should not be expressed due to the absence of galactose.

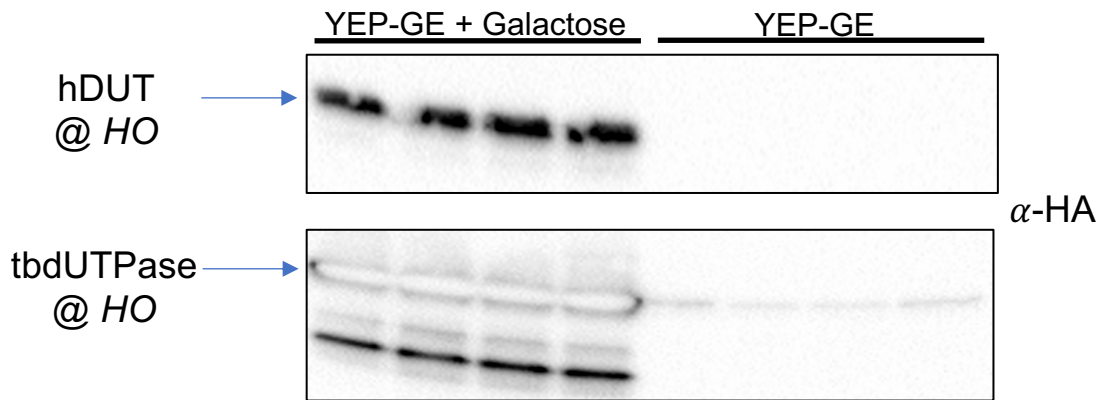


Figure 11: Western blot showing expression of HA tagged hDUT and tbdUTPase proteins. hDUT (top) and tbdUTPase (bottom) genes were integrated into the yeast genome at the HO locus followed by Western blots to confirm expression. The new strains were grown in YEP-GE 2% galactose media allowing for their expression. Bands for tbdUTPase are shown white when the image was captured because the gel was overloaded with the extract collected. Bands present below tbdUTPase is most likely the degraded tbdUTPase protein.

After confirming expression, next I tested if the dUTPase genes integrated into the yeast genome in the strain YNK425 would give the expected results: when grown in YEP-GE with auxin both strains with hDUT and tbdUTPase should show significant inhibition of growth because the endogenous yDUT1-AID will be degraded and galactose is not present to induce the expression of hDUT and tbdUTPase. Inversely, when grown in YEP-GE 2% galactose media with auxin the strains should exhibit no inhibition in growth, because although auxin's presence causes the endogenous yDut1-AID to degrade, the expression of hDut and tbdUTPase is induced due to the presence of galactose ultimately showing functional complementation. Functional complementation of these new strains was tested by creating growth curves (**Figure 12**). The following statements about Figure 12 apply to both hDUT (top graph) and tbdUTPase (bottom graph). When *ydut1-AID* strain (YNK425) is treated with 500 μ M auxin in both YEP-GE and YEP-GE-galactose (YEP-GE-Gal) the growth is significantly inhibited as expected. When human and *T. brucei* dUTPase genes were added and grown in YEP-GE, they do not show any signs of inhibited growth in the presence of auxin, even though they are expected to

behave similarly to YNK425 since galactose is not present to induce the expression of the dUTPase gene. When grown with galactose in the presence of auxin, the strain grows similarly to when auxin is not present, which suggests that the human and *T. brucei* dUTPase genes may be able to functionally complement when the native yDut1-AID is degraded. However, since the new strains did not have growth inhibition in the presence of auxin when grown in only YEP-GE, that functional complementation does not appear to be actually occurring.

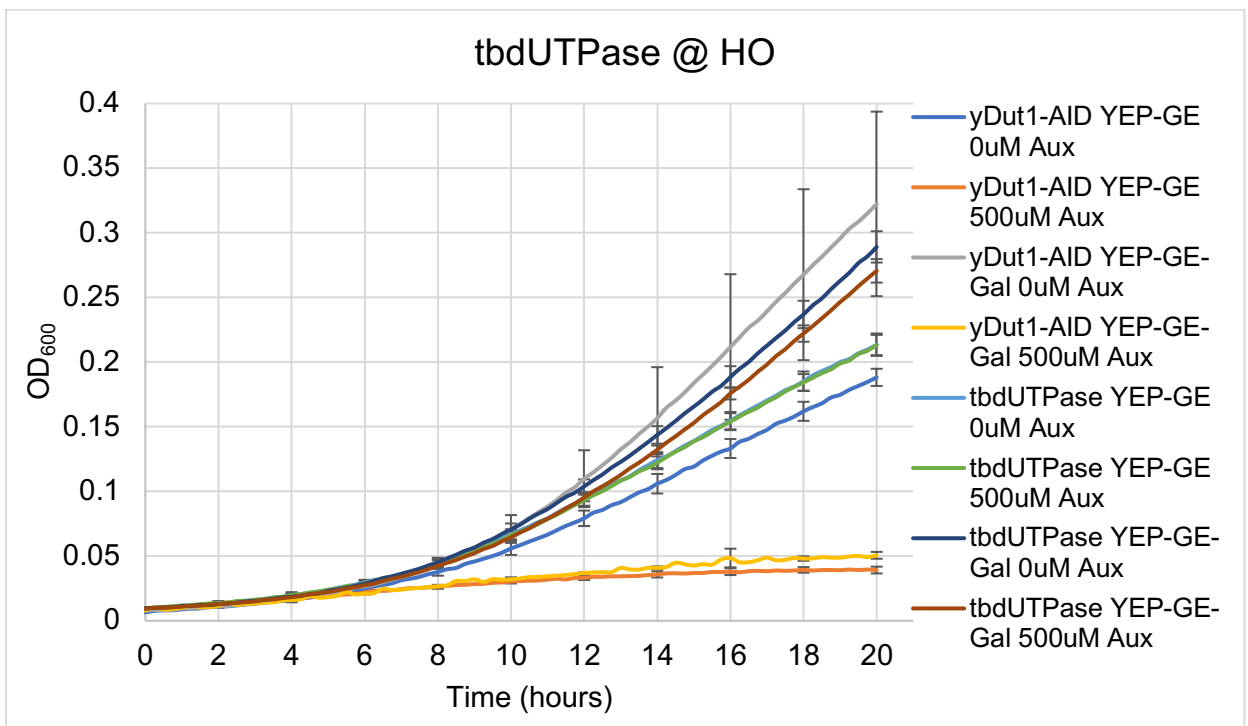
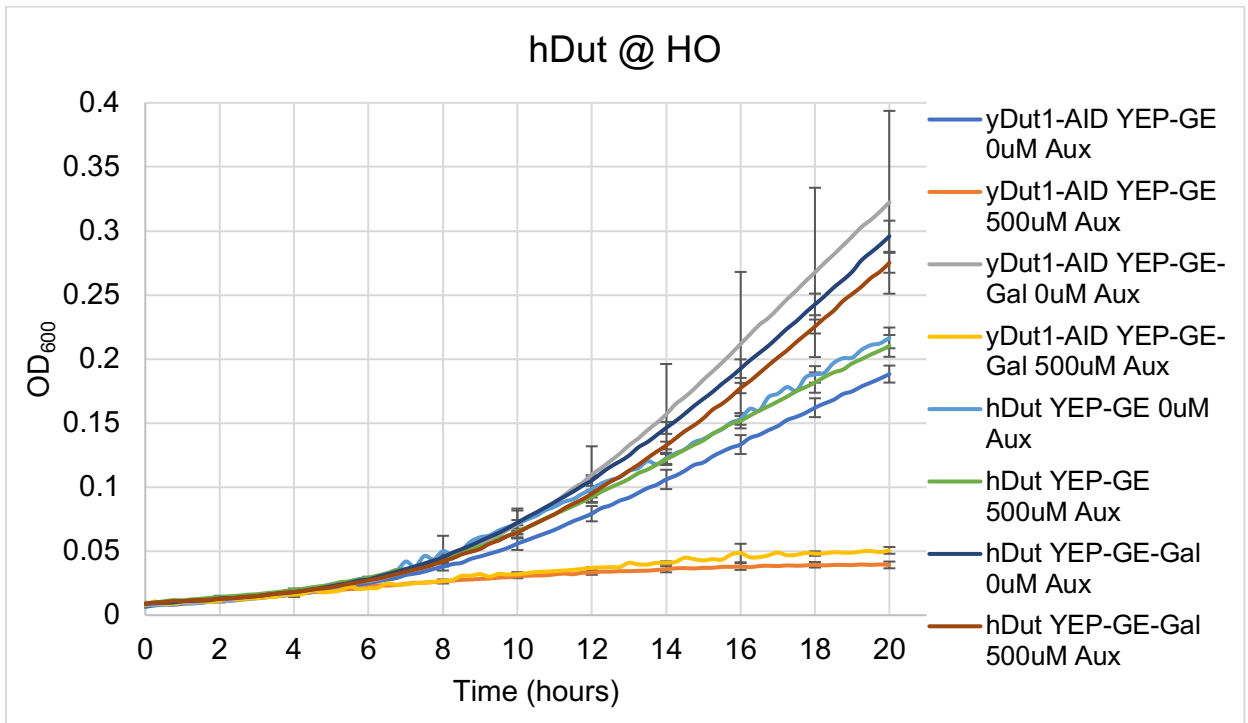


Figure 12: Growth curves testing functional complementation of hDUT and tbdUTPase genes integrated into the yeast genome in the *HO* gene. hDUT (top) and tbdUTPase (bottom) genes were integrated into the yeast genome and tested for functional complementation in the presence of galactose and 500 μ M auxin via growth curves.

To check if the result shown in Figure 12 is possibly functional complementation, a negative control was created that mimicked the integration of a dUTPase gene into the *HO* locus. For the negative control, the same plasmid consisting of tbdUTPase under the control of pGal, a *URA3* marker, and flanking *HO* sequences was cut using the restriction enzyme *SpeI*. Within the tbdUTPase sequence, *SpeI* is capable of cutting at two locations, which allowed a significant portion of the gene to be removed and the plasmid was religated, creating a plasmid containing an inactive tbdUTPase gene. This plasmid was transformed into YNK425 and the addition of the inactive tbdUTPase gene into the *HO* gene was confirmed with PCR (data not shown). The growth of this new strain, YNK760 (now referred to as 'Neg' for negative control) was tested by creating growth curves (**Figure 13**). The Neg strain was grown alongside YNK425 and is expected to grow similarly to it in both YEP-GE and YEP-GE with galactose in the presence and absence of 500 μ M auxin. In both mediums, we observed that, when Neg is grown with 500 μ M auxin, it does not show any signs of growth inhibition. Because we failed to demonstrate the growth inhibition of the Neg strain in the presence of auxin, we do not have the proper control to demonstrate that the expression of hDUT and tbdUTPase in the presence of galactose could be complementing the absence of the native yDut1.

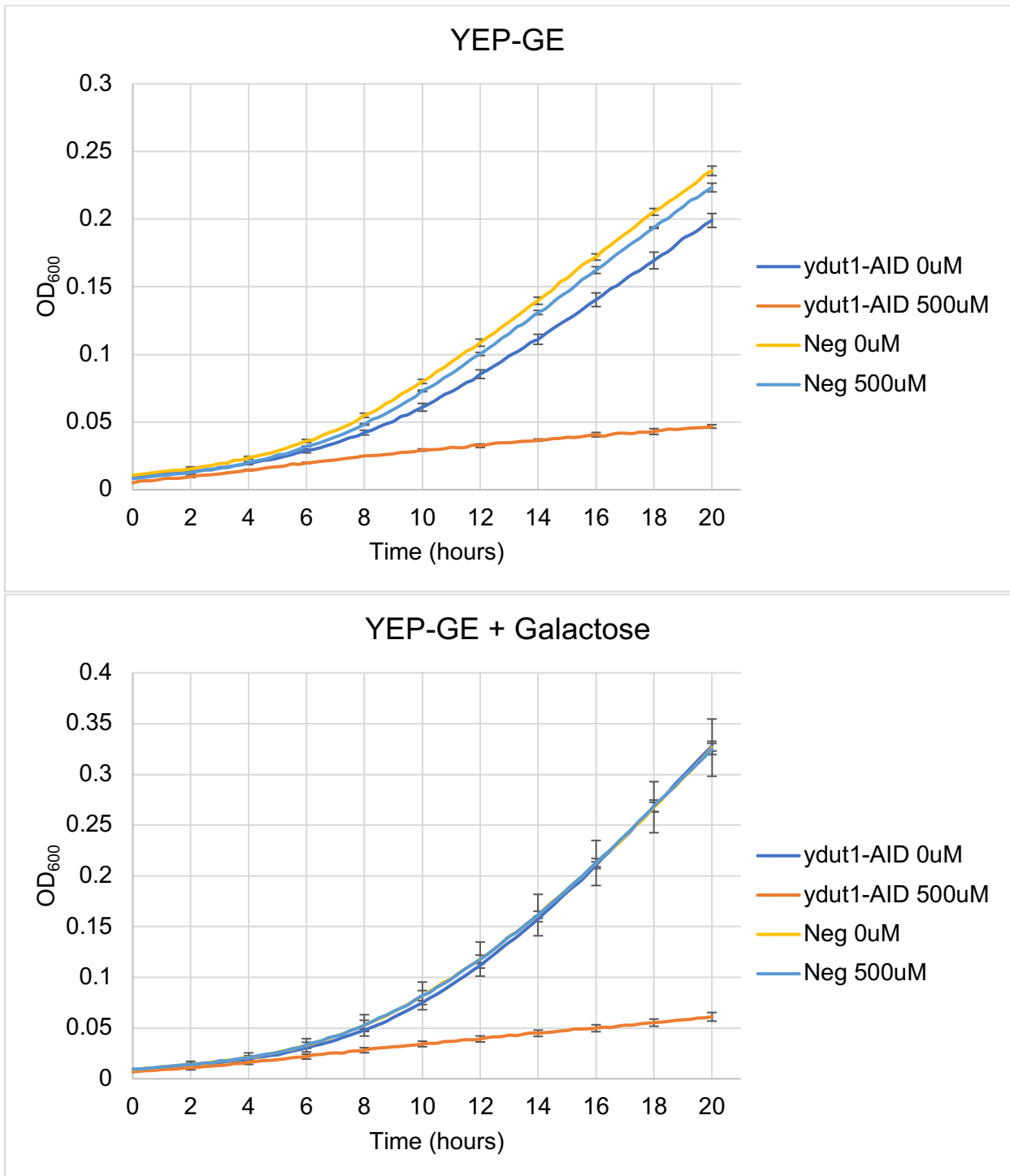


Figure 13: Growth curves showing growth behavior of inactive *tbdUTPase* integrated into the *HO* gene.

YEP-GE (top) and YEP-GE with galactose (bottom) mediums were used to grow YNK425 and Neg strains with and without 500 μ M auxin. Inactive *tbdUTPase* gene was integrated into the *HO* gene of YNK425 to create the Neg strain.

This outcome led us to question whether or not the endogenous yDUT1-AID was being degraded in these newly created strains with new dUTPase genes. Similar to Figure 7, Western blots were carried out to monitor the degradation of the 3X-Flag tagged *ydut1-AID* (**Figure 14**). Two sets of cell extracts were collected at three timepoints, 0, 1, and 2 hours, one set without auxin and the other with 500 μ M auxin. As shown in Figure 15, over the course of the two hours, the endogenous *ydut1-AID* protein in the original YNK425 degrades in the presence of auxin. However, in strains with the integration of *hDUT*, *tbdUTPase*, or Neg cassette at the *HO* locus, the endogenous *ydut1-AID* is not degraded when treated with 500 μ M auxin. The integration of the dUTPase sequences into the yeast genome seems to somehow interfere with AID system, no longer allowing for *ydut1-AID* to be degraded. Overall, the methods and experiments mentioned here were not able to prove complementation did in fact occur. Therefore, other experiments were conducted as an alternative method to target *T. brucei* dUTPase with a small molecule.

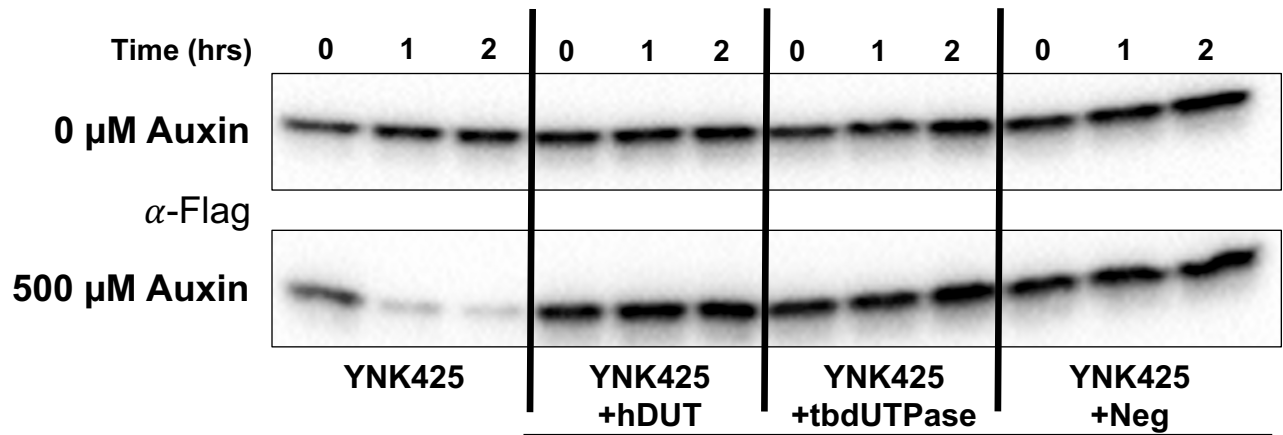


Figure 14: Western blot tracking the degradation of endogenous ydut1-AID. Cell extracts were collected at 0, 1, and 2 hour timepoints to create a Western blot showing the degradation of the 3X-Flag tagged endogenous yDut1 when treated without auxin (top) and when treated with 500 μM auxin (bottom).

3.3 High throughput virtual screen for *T. brucei* dUTPase ligands using Schrödinger's suite

Significant structural differences exist between human and *T. brucei* dUTPase proteins suggesting that it would be feasible to find a small molecule inhibiting the function of *T. brucei* dUTPase with little effect on human dUTPase. Since we were not able to set up complementation system using *S. cerevisiae* as a model system, which would have been a necessary tool in screening for such small molecule in vivo, an alternative method to perform a drug screen is a virtual or computational approach. This component of the project was made possible thanks to the collaboration with Dr. John Tainer at MD Anderson Cancer Center who provided us access to the software and the virtual drug screen was performed by Dr. Nayun Kim. With crystal structures available online from other studies of human and *T. brucei* dUTPases, a virtual drug screen was performed utilizing Schrödinger's Suite. Being able to conduct a virtual drug screen rather than a physical one in multiple-well plates is a much faster and efficient process, allowing for thousands of small molecules available online to be tested with the protein of desire [33]. In our case, we know the best fitting molecule that binds to the binding pocket of the dUTPases is dUTP/dUMP (**Figure 15**). Therefore, small molecules that are similar in structure to dUTP/dUMP would be the best candidates for the purpose of this project.

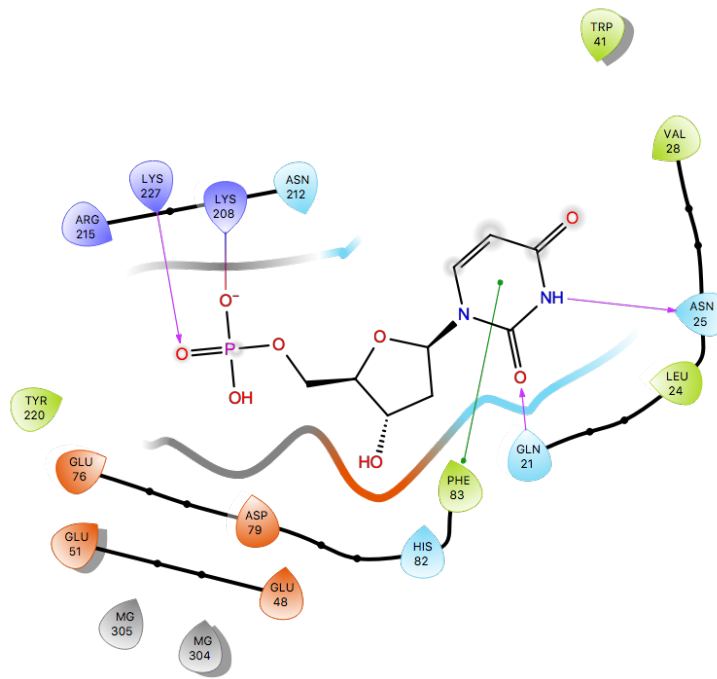


Figure 15: *T. brucei* dUTPase residues interacting with dUMP.

This interaction map was generated using PyMol software. dUTPase cleaves off a pyrophosphate from dUTP, leaving behind dUMP, which can be used in the thymidine biosynthesis pathway.

To begin the virtual screen, ligands to be screened needed to be narrowed down from the thousands available through the online database. Our goal was to identify a small molecule that binds to *T. brucei* dUTPase to inhibit its function but does not bind to human dUTPase. For the HTVS, a custom library of 5000 compounds (called “Tainer 5000”) was selected from the Life Chemical library based on their variety, low toxicity, small molecular weights, and drug-like properties. This library was generated by the lab of John Tainer at MD Anderson to use in screening for ligands that bind to DNA or nucleotide-interacting proteins. Once molecules that bind to *T. brucei* dUTPase have been found, they can then be tested to see which ones do not fit the human dUTPase, which is what we desire. The 1.47 Å resolution *T. brucei* dUTPase structure (PDB ID: 4DK2) [25] was uploaded to the Glide program. In order to screen for ligands that bind to the catalytic pocket of dUTPase, the “Search Space” was defined as the annotated catalytic center where dUTP/dUMP binds. The dUTPase requires a magnesium cation (Mg²⁺) to be enzymatically active [40]. Several charged residues (Q21, N25, E48, E51, R215, K227) involved in hydrogen bonding with PO₄ and Mg²⁺ are located in the catalytic core in addition to several aromatic residues (W41, T76, H82, F83, Y220). For the virtual screen, the software allowed us to also include magnesium with the dUTPase crystal structure to have a more accurate representation of the protein. One caveat of performing a drug screen in this manner is the crystal structure of our target protein is in a static state, whereas proteins are always in a dynamic state, which may lead to more molecules being predicted to be positive hits in the screen [41].

From the virtual docking simulation of the Tainer 5000 library to the catalytic pocket of TbdUTPase, over 1000+ molecules were predicted as positive hits (docking score <-6.5; MMGBSA dG bind <-20) (**Figure 16**). These molecules were plotted as docking score vs. MMGBSA dG Bind. The docking score indicates how

well the molecule binds or fits into the binding pocket of the protein structure in question. The MMGBSA dG Bind can also be referred to as “free energies of binding”, which indicates how strong of a bond there is between the molecule and protein structure in question. In addition, the measurements are in log scale, therefore, the more negative the values are for a molecule, the better it fit into the binding pocket with a greater binding strength. The virtual docking of Tainer 5000 library was repeated using the annotated structures of human DUT (PDB ID: IQ5U and 3ARA) [35, 36]. From the positive hits from docking to the tbdUTPase structure, we eliminated any positive hits to the hDUT in order to find a ligand specific to tbdUTPase but not to hDUT. The list was narrowed down to 13 molecules by 1) prioritizing lower MMGBSA dG Bind and docking score, 2) selecting only one among ligands with very similar structures, and 3) prioritizing molecules with structural similarity to nucleotides (**Table 6**).

These 13 molecules were provided to us by Dr. John Tainer. Among the 13 molecules, only one had been previously characterized as a drug, #7, carbamazepine. This is a common anticonvulsant drug that is widely used to control seizures [42]. Anticonvulsants are commonly used for brain disorders [43], thus must penetrate into the blood-brain barrier in order to be effective. Since *T. brucei* infection at its second stage does get into blood-brain barrier as well, carbamazepine is a well-suited molecule to potentially target and inhibit the function of *T. brucei* dUTPase regardless of the stage of the disease. Carbamazepine also is a well-studied drug and therefore would not require more studies such as toxicity analysis. With 13 candidate molecules finalized, these molecules can now be further used to study their effect on yeast, human and *T. brucei* dUTPase.

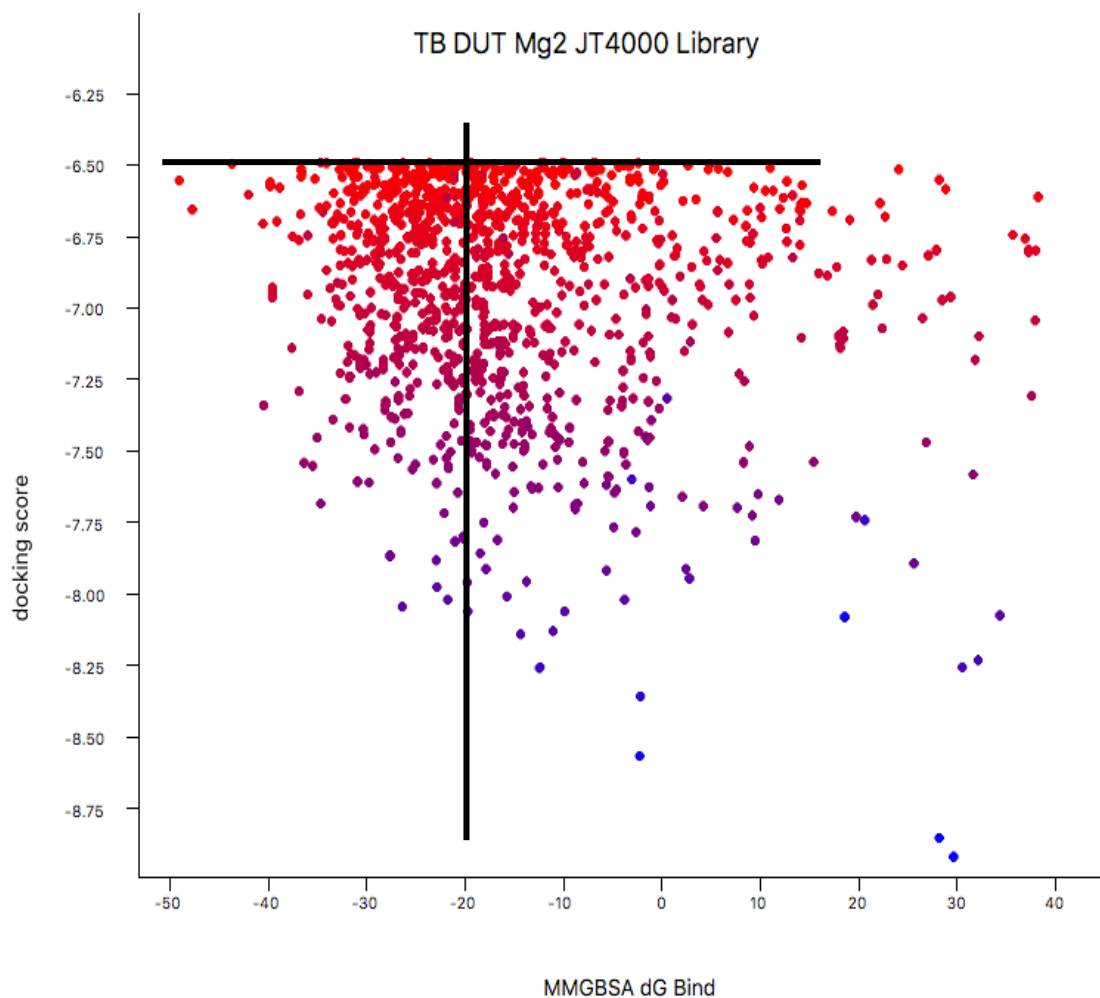


Figure 16: HTVS result showing positive binding hits for *T. brucei* dUTPase. This figure shows the results of the HTVS. *T. brucei* dUTPase was tested with the presence of magnesium. The y-axis, docking score, indicates how well ligands fit into the binding pocket of the structure and the x-axis, MMGBSA dG Bind, indicates how strong the binding is.

Table 6: 13 molecules narrowed down by HTVS.

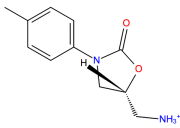
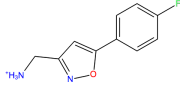
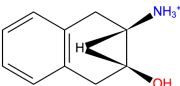
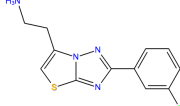
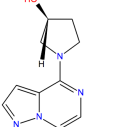
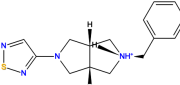
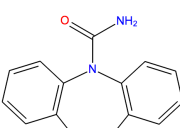
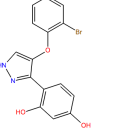
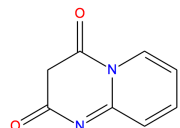
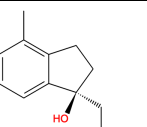
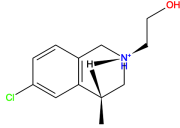
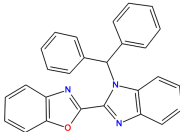
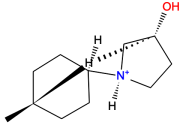
Molecule #	ID Number	Name	Structure
1	F2147-0060	5-(aminomethyl)-3-(4-methylphenyl)-1,3-oxazolidin-2-one	
2	F2162-0006	[5-(4-fluorophenyl)-1,2-oxazol-3-yl]methanamine	
3	F1905-0500	3-amino-1,2,3,4-tetrahydronaphthalen-2-ol	
4	F2189-0253	2-[2-(3-fluorophenyl)-[1,3]thiazolo[3,2-b][1,2,4]triazol-6-yl]ethanamine	
5	F6541-4753	1-pyrazolo[1,5-a]pyrazin-4-ylpyrrolidin-3-ol	
6	F6546-0690	3-(2-benzyl-1,3,3a,4,6,6a-hexahydropyrrolo[3,4-c]pyrrol-5-yl)-1,2,5-thiadiazole	
7	F0348-2551	Carbamazepine	
8	F3385-1587	4-[4-(2-bromophenoxy)-1H-pyrazol-5-yl]benzene-1,3-diol	
9	F1516-4482	pyrido[1,2-a]pyrimidine-2,4-dione	
10	F9994-0418	1-(aminomethyl)-4-methyl-2,3-dihydroinden-1-ol	

Table 6. Cont.			
Molecule #	ID Number	Name	Structure
11	F0916-0420	2-(6-chloro-4-methyl-3,4-dihydro-1H-isoquinolin-2-yl)ethanol;hydrochloride	
12	F1364-0012	2-(1-benzhydrylbenzimidazol-2-yl)-1,3-benzoxazole	
13	F6541-4740	1-(4-methylcyclohexyl)pyrrolidin-3-ol	

3.4 *T. brucei*/yeast viability testing with molecules found from the high throughput virtual screen

With the 13 molecules found that virtually bind to *T. brucei* dUTPase, but not to human dUTPase, I next proceeded to see if any one of the molecules had a direct growth-inhibitory effect on *T. brucei* cells. Since these molecules likely bind to dUTPase, an essential enzyme, if one of them binds and inhibits the function of dUTPase in *T. brucei*, then those cells will no longer be viable and there should be a significant increase in cell death. I was taught by Dr, Kyu Lee, a postdoc in Dr. Ziyin Li's lab, to grow cultures of *T. brucei*, so that I could perform these tests.

A stock culture of a blood-stream form *T. brucei* was started and was replenished with fresh medium when the stock culture was nearing its saturation point (approximately every 2 days). All of the 13 molecules were dissolved in DMSO, therefore I first tested different percentages of DMSO, which would be used as a negative control, to see if they were toxic to *T. brucei* cultures. The optimal, non-cytotoxic DMSO percentage to use for the cultures was determined to be 0.5% (data not shown). Final concentrations of 10 μ M for the 13 molecules and MTX, which was used as a positive control since it inhibits the essential thymidylate synthesis pathway, were added to the *T. brucei* cultures. When diluting the molecules into the cultures, the concentrations of DMSO in the 48-well plate being used was approximately 0.3%, therefore, more DMSO was added to reach the final concentration of 0.5% to match the negative control. All cultures started with an initial concentration of 5×10^4 cells/mL and cells were counted daily for 4 days with a hemocytometer. Due to the great amount of time it would take to count all the cells for a total of 15 samples and risk of leaving *T. brucei* cultures out of the incubator too long, the molecules were split up into 4 different sessions (**Figure 17**). MTX treatment led to significant signs of cell death whereas the control, (ctrl in Figure 17), showed normal growth. Of the 13 molecules, molecule #4 led to significant cell

death to the level similar to MTX-induced cell death. Molecule #5 showed a negative cell growth rate from day 3 to day 4, which may indicate a delayed effect of cell killing. Unfortunately, no other molecule showed any signs of growth inhibition. Molecule #4 may be able to kill *T. brucei* by binding to dUTPase and inhibiting its function, based on the virtual screen result.

Next, I determined if molecule #4 is a generally toxic molecule and would be harmful to yeast cells. The same 13 molecules listed in Table 6 were tested on the yeast strain YNK421 with wild type *DUT1* using the plate growth assay. I first determined what percentage of DMSO is safe to use for YNK421. 0.5% DMSO was determined to not affect cell growth of YNK421 (data not shown). The 13 molecules were again tested at the concentration of 10 μ M but MTX this time was increased to 500 μ M because 10 μ M of MTX did not sufficiently inhibit yeast cell growth. Due to space on the 96-well plate, the 13 molecules were split into two different plate reader runs (**Figure 18**). Molecule #4, which inhibited the growth of *T. brucei*, presumably by inhibiting the function of dUTPase, had no effect on the growth of yeast. From this, it can be concluded molecule #4 does not inhibit yeast dUTPase and therefore, it most likely would also have no effect of human dUTPase, which is highly homologous to the yeast protein. And, molecule #5, which partially inhibited the growth of *T. brucei*, did not affect yeast cell growth.

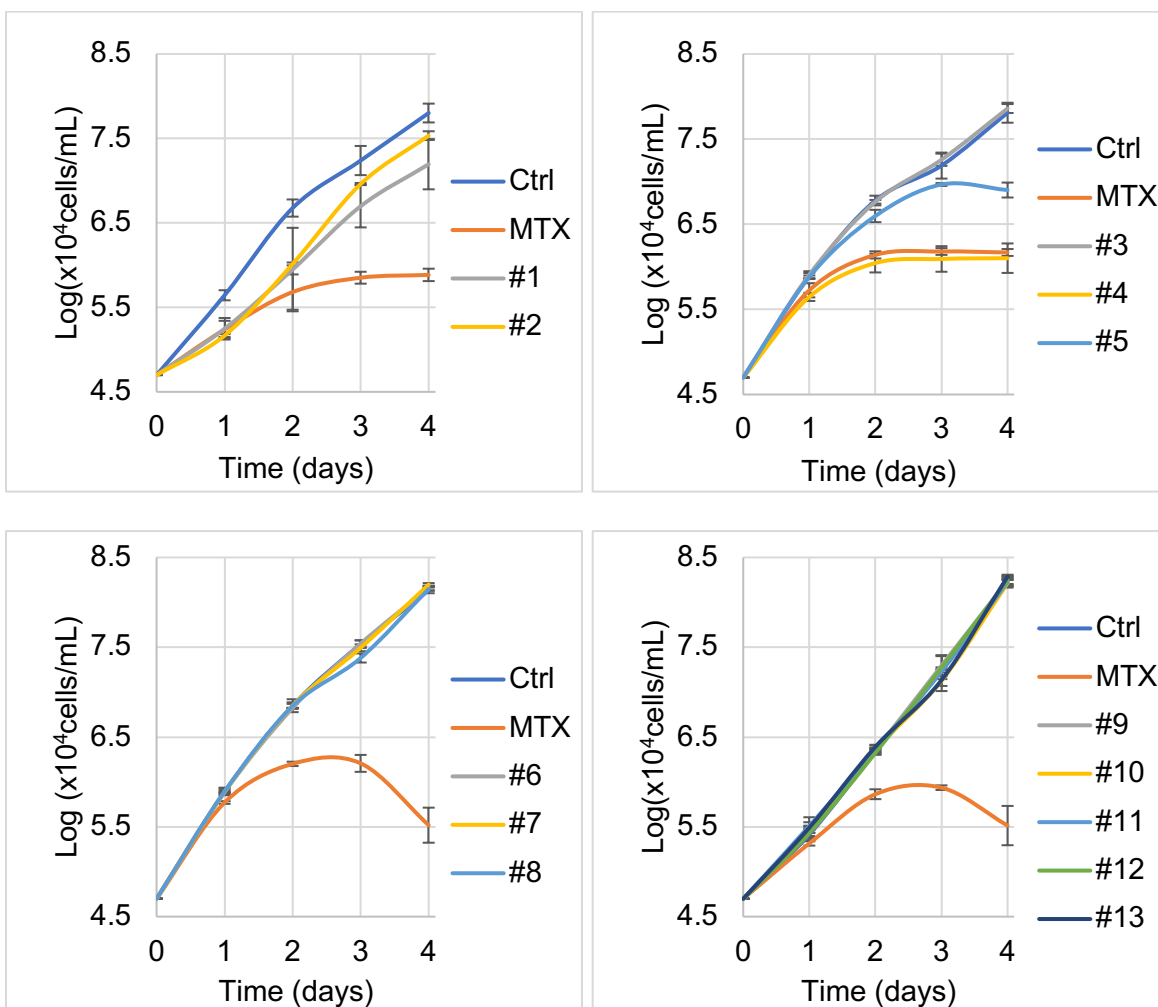


Figure 17: Growth curves testing the effect of molecules 1-13 on *T. brucei*. *T. brucei* blood-stream form cultures were grown in triplicates testing the effect of molecules 1-13 on growth. All samples contain a final 0.5% DMSO and all molecules are at a final concentration of 10 μ M in the 48-well plate.

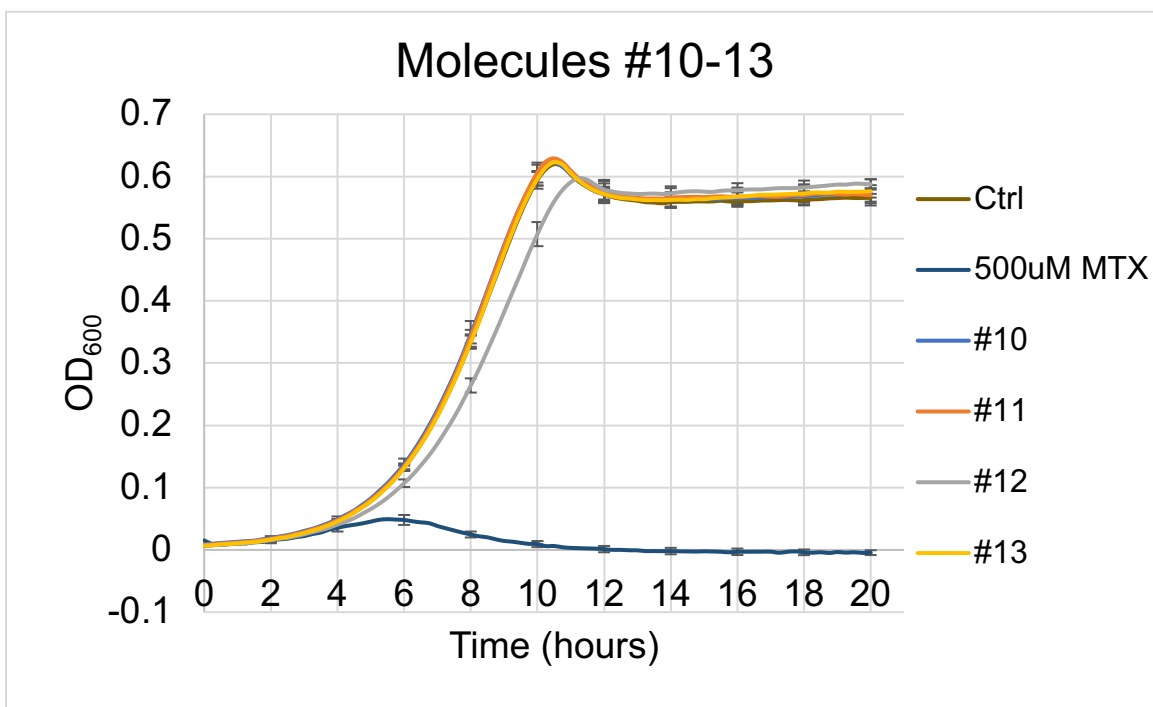
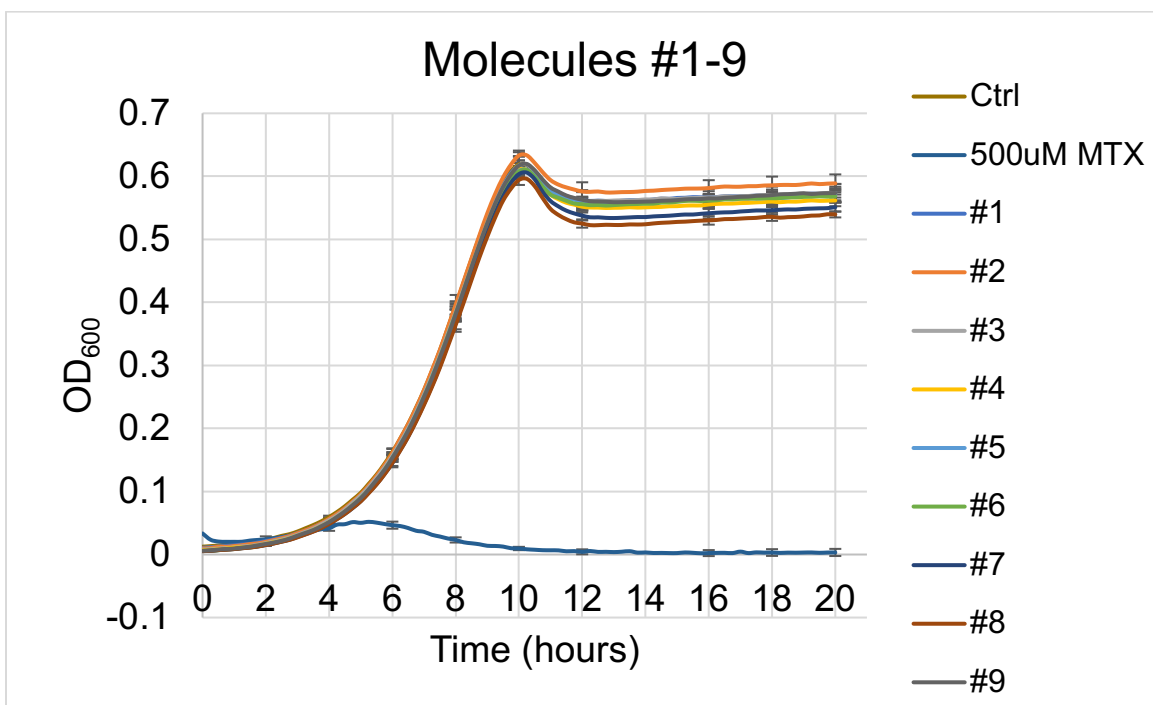


Figure 18: Growth curves testing the effect of molecules 1-13 on YNK421. Growth curves were generated using a plate reader to test the effect of molecules 1-13 on YNK421 growth. All samples contain 0.5% DMSO and all molecules were tested at a final concentration of 10 μ M. 0.5% DMSO was the negative control and MTX was the positive control at 500 μ M. N=7.

3.5 Overexpression and purification of yeast, human, and *T. brucei* dUTPase proteins

In order to test whether the candidate ligands found through HTVS would inhibit *T. brucei* dUTPase, but have no effect on human and yeast dUTPases, we overexpressed and purified the dUTPase enzymes to directly test the enzymatic activity in the presence of candidate molecules. Creation of plasmids containing hDUT and tbdUTPase and their transformation into BL21 cells, along with a vector as a control, is described under Protein Purification in the Materials and Methods. First, overexpression after adding IPTG was confirmed for all of the following proteins before proceeding to protein purification: yDUT1, hDUT, tbdUTPase #1, tbdUTPase #2, and vector (data not shown). **Figure 19** shows the results of the protein purification process. For hDUT, tbdUTPase #1, and tbdUTPase #2, the proteins were overexpressed, and a large amount of purified protein was eluted. All bands for the purified proteins were the expected size: yDUT1 approximately 15 kDa, hDUT approximately 17 kDa, and tbdUTPase approximately 28 kDa. The purification of the vector does not contain any prominent bands. The other prominent bands that are present with hDUT and both tbdUTPase purifications could possibly be multimers of the proteins. yDUT1, hDUT, and tbdUTPase #1 were also sent for mass spectrometry to confirm these bands were the correct protein (data not shown).

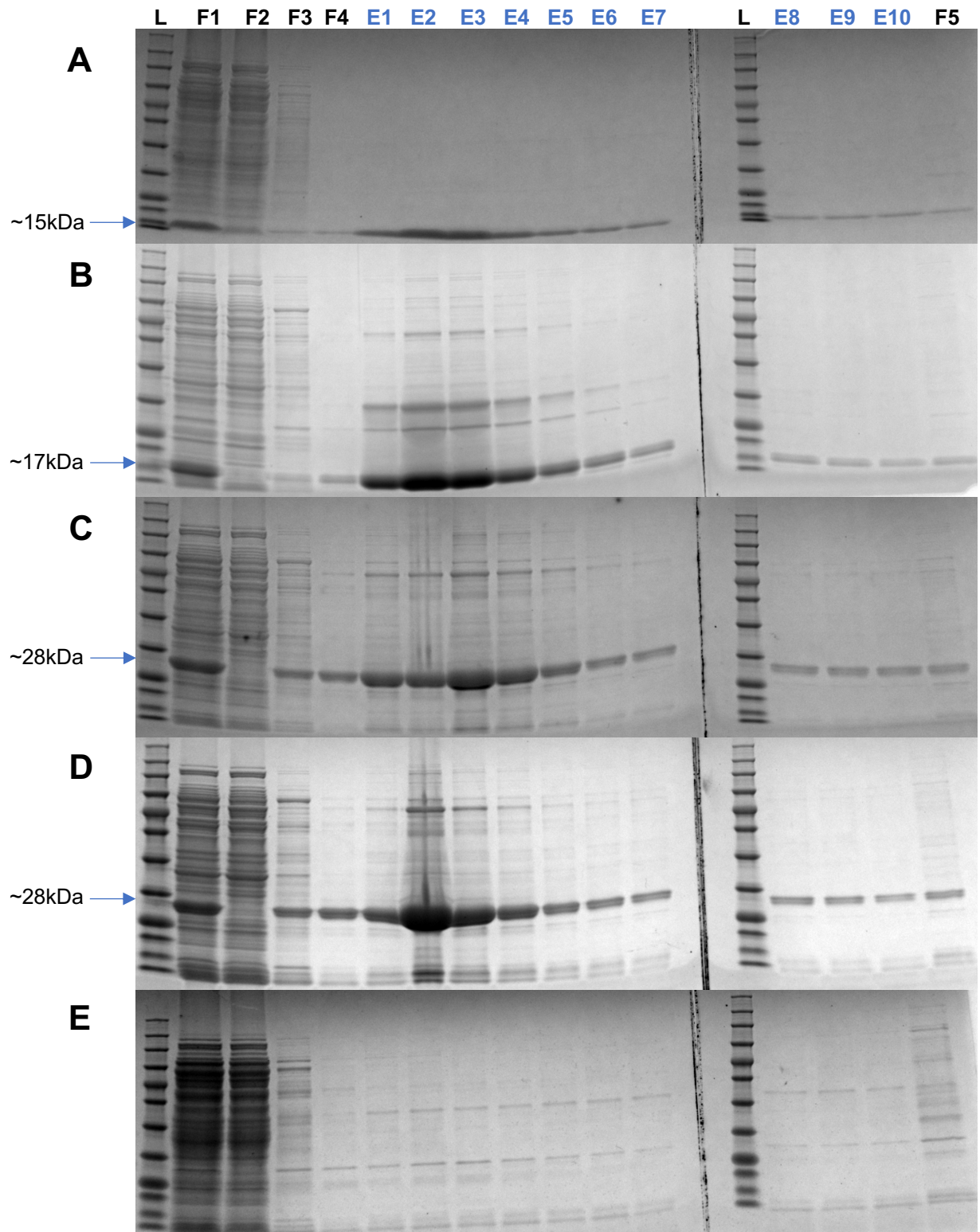


Figure 19: Protein purification results of collected fractions and elution. Protein staining results for the collected fractions and elution of **A)** yDUT1, **B)** hDUT, **C)** tbdUTPase #1, **D)** tbdUTPase #2, and **E)** vector. 5 μ L of each sample was applied to the gel. The following states what each of the lanes represent. L: ladder, F1: cell lysate, F2: column flow through, F3: wash #1 with 50 mM imidazole, F4: wash #2 with 80 mM imidazole, E1-E10: elution aliquots with 500 mM imidazole, F5: leftover resin in column.

After the elution fractions were checked by electrophoresis and Coomassie Blue staining, elution fractions 7-10 from each purification were collected and combined for each. The combined fractions were then transferred to storage buffer and stored in 100 μ L aliquots as described in the Materials and Methods section. **Table 7** shows the concentrations of the purified proteins calculated using a protein quantification kit. **Figure 20** shows the Coomassie-stained protein images of stored fractions. With this successful protein purification, these proteins' enzymatic activity could be tested to see if molecule #4 is dUTPase specific.

Table 7: Protein concentrations of purified proteins.

Protein	yDUT1	hDUT	tbdUTPase #1	tbdUTPase #2	vector
Concentration (mg/mL)	0.353	0.073	0.116	0.089	0.012

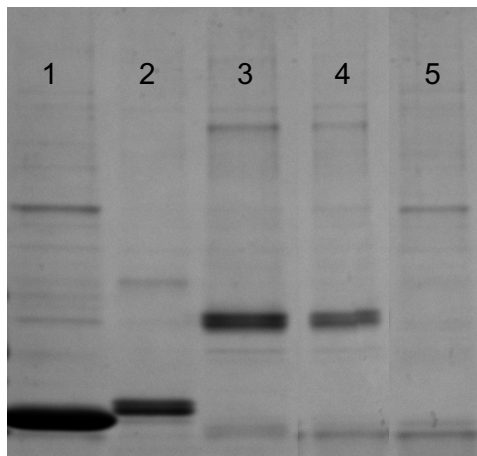


Figure 20: Final protein staining image of purified proteins.

5 μ L of each final aliquoted protein was run, showing the degree of purity. The following states what each lane represents. Lane 1: yDUT1, Lane 2: hDUT, Lane 3: tbdUTPase #1, Lane 4: tbdUTPase #2, and Lane 5: vector.

3.6 Enzymatic activity of dUTPase proteins

I observed that *T. brucei* cells were killed in the presence of molecule #4, however, it was important to determine if the effect is due to specific inhibition of dUTPase activity. In order to address this, dUTPase proteins (yeast, human, and *T. brucei*) were purified. A protein extract from *E. coli* cells transformed with empty vector was subjected to the same purification protocol and serves as the negative control (referred to as “vector”). dUTPase’s function is to convert dUTP to dUMP and, in that process, a pyrophosphate, PPI, is generated as a by-product. The generation of PPI can be measured to determine the enzyme’s activity. The PiPer Pyrophosphate Assay Kit measures the generation of PPI by first converting it to an inorganic phosphate, Pi. Pi can be detected in a series of reactions ultimately leading to the generation of resorufin, a redox probe, which emits a fluorescent signal that can be measured with a plate reader. Following the kit’s protocol, several runs were performed testing the enzymatic activity of the five purified proteins (**Table 8**). The kit calls for generating a standard curve by making dilutions of the provided pyrophosphate standard and then back calculating the amount of pyrophosphate generated by the enzyme in question. Unfortunately, every time this assay was performed, the standard provided with the kit did not result in the appropriate fluorescent values to generate a proper linear curve and the amount of pyrophosphate generated could not be calculated. Furthermore, every time this assay was run, it seemed that yDut1 and hDUT were active enzymes but tbdUTPase #1 and #2 were not active. The tbdUTPase fluorescence values are not significantly different from the negative control. Thus, it appears that tbdUTPase is not enzymatically active. In addition, the vector’s fluorescence, which is expected to be similar to the negative control, was significantly lower. Due to the assay not working as expected, the purified proteins could not be tested to determine if molecule #4 affects their activity.

Table 8: PiPer Pyrophosphate assay experiment.

Sample	Fluorescence	Standard Deviation
PPi 100 μ M	193.5	18.84
PPi 50 μ M	201	6.78
PPi 25 μ M	179	20.05
PPi 12.5 μ M	169.5	9.47
PPi 6.25 μ M	141.75	16.07
PPi 3.125 μ M	123.5	12.07
Negative Control	92.25	0.96
Positive Control	657.5	47.68
yDut1	159.25	5.12
hDUT	148.75	6.24
tbdUTPase #1	88.5	3.42
tbdUTPase #2	95.25	7.63
vector	51.75	1.71

The inconsistent results with the PiPer Pyrophosphate Assay Kit led me to use an alternate method to measure the enzymatic activity of dUTPase. It is well known dUTP (U) can be incorporated into DNA and dUTPase is responsible for inhibiting this by converting dUTP to dUMP. Based on this property, we used a PCR-based assay to test the activity of dUTPase and the effect of candidate molecules #4 and #5. When nucleotides dATP, dTTP, dCTP, and dGTP (A, T, C, and G) are used to form a PCR product, the PCR product can be visualized via gel electrophoresis. The same can be done by using nucleotides A, U, C, and G since U can be added to DNA in lieu of T. When a nucleotide is missing, then no PCR product will form because the amplification cannot occur completely without the missing nucleotide. When A, C, G, along with either T or U, are used for PCR and U has been incubated with a dUTPase before the reaction, U as dUTP will have been degraded to dUMP, which cannot be incorporated into DNA resulting in no PCR product formed. When T is incubated with dUTPase, it should have no effect on PCR efficiency since dUTPase is specific for U. PCR was performed using T7 (TAATACGACTCACTATAGGG) and M13Rev (CAGGAAACAGCTATGAC) primers and using pGPD2, an arbitrary plasmid, as a template. In addition, each PCR reaction contained 5 μ L of purified dUTPase protein and 0.3% DMSO. The PCR reactions were repeated with either Taq DNA polymerase or MyTaq DNA polymerase (modified and licensed product of Bioline).

Figure 21 shows the results of the PCR-based enzymatic activity assay. Both molecules #4 and #5 were tested. For either DNA polymerases used, the controls resulted in the proper PCR products forming as expected. Lanes 1 and 2 in both Figures 21A and 21B show a very prominent band forming when individual nucleotides are used and U incorporated into DNA can still form a PCR product. Lane 3 shows when missing a nucleotide, missing T/U, results in no formation of a PCR product due to incomplete PCR. Lanes 4-8 consist of T nucleotide incubated with water or one of the four purified proteins. For each lane a prominent band is

present as expected because dUTPase does not affect dTTP (T). In Figure 21B, bands in lane 5 are less visible when using MyTaq DNA Polymerase which may be due to pipetting error. Lane 9 is another control where U incubated with water should have no effect on PCR product formation. For Lanes 10 and 11 with DMSO only, yDut1 or hDUT should degrade dUTP leading to no PCR product formation. Similar results with no PCR product were expected when molecule #4 or #5 are added since these molecules are not expected to inhibit yeast or human enzymes. For lane 12 where dUTP was treated with TbdUTPase prior to PCR reaction, PCR product was either significantly reduced (with Taq polymerase) or absent (with MyTaq polymerase) indicating that tbdUTPase actively degraded dUTP. For the reaction in lane 12 in the presence of molecules #4 and #5, more prominent PCR products are expected if either of these molecules inhibit tbdUTPase, so that dUTP is not degraded to dUMP. However, as shown in in lane 12 of Figure 21A, PCR band is significantly less present for molecule #4 and not visible at all for molecule #5. For Figure 21B, bands are not present for both molecules #4 and #5 in lane 12. This indicates that molecules #4 and #5 may not be dUTPase specific and the killing of *T. brucei* cells exhibited in Figure 17 may be due to another pathway being affected. Lane 13 consisting of the vector control shows prominent bands present as expected due the absence of dUTPase proteins. Overall, the enzymatic assays performed failed to show that molecule #4 or #5 is an inhibitor of dUTPase.

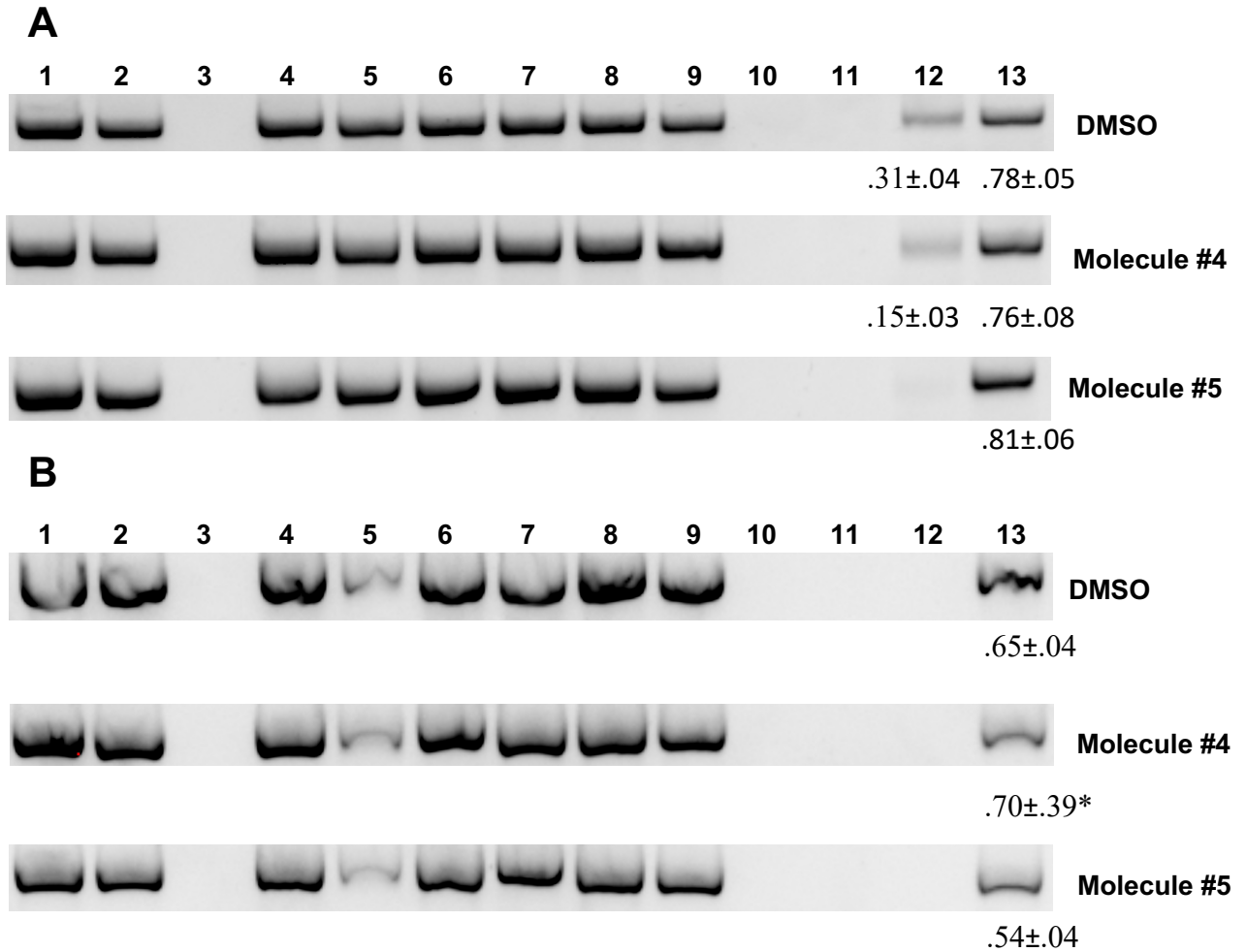


Figure 21: PCR-based dUTPase enzymatic activity assay.

Plasmid pGPD2 was used as a template to amplify the approximately 1 kb region between T7 and M13Rev primers. PCR products were run on 1% agarose gel and stained with SYBR-Green. **A)** PCR reactions using Taq DNA Polymerase and **B)** PCR reactions using MyTaq DNA Polymerase. For both A and B, the table below states what each lane contains. Lanes 4-13 all contain A, C, and G as well as in addition to T or U as indicated. Reactions either contained DMSO, molecule #4, or molecule #5 as indicated on the right of the gel picture. The PCR reactions shown are only a single replicate from a set of three individual reactions. The average band intensity below lanes 12 and 13 is calculated in reference to Lane 9; *the quantification for Molecule #4 under **B** is an average of 2 replicates.

1: A T C G	4: T incubated with H ₂ O	9: U incubated with H ₂ O
2: A U C G	5: T incubated with yDut1	10: U incubated with yDut1
3: A C G	6: T incubated with hDUT	11: U incubated with hDUT
	7: T incubated with tbdUTPase #2	12: U incubated with tbdUTPase #2
	8: T incubated with vector	13: U incubated with vector

Chapter 4: Discussion

Using *S. cerevisiae* as a model system is an effective and efficient method to perform a pharmacological study [44]. Yeast is an easy to manage organism and experiments can be performed relatively quickly and provide the ability to replicate results more productively in comparison to other organisms. For the purpose of this project, yeast was to be used as a model system to express and study the essential enzyme dUTPase of the parasite *T. brucei* and also of humans. This is ideal because yeast is widely used as a model organism to test functions of human genes and enzymes [45]. In this case, a drug screen would have been performed to find a molecule that inhibits the function of the dUTPase from *T. brucei*, but would have no effect on human dUTPase, along with no effect on yeast itself. Having no harmful effect on yeast may indicate the found molecule(s) may not be toxic to human cells as well due to their similarities. Unfortunately, I was not able to use yeast as a model system to demonstrate functional. That is, the tests performed were not able to prove that, when human or *T. brucei* dUTPases were added to the yeast genome, they functionally complement the absence of endogenous Dut1 in the strain YNK425 in the presence of auxin.

Due to the fact that a physical drug screen could not be performed with yeast cells containing human and *T. brucei* dUTPase, we chose to perform a virtual drug screen. The Glide platform allowed for thousands of molecules available through their online database to be screened against tbdUTPase. The HTVS screen is the fastest screening tool in the software, which does leave room for error in terms of finding the right molecule and may have led to extra positive hits. However, because we also needed to determine if those molecules bound to hDUT, we allowed for a more stringent screen to be performed. The 13 molecules were found that fit our criteria of 1) binding to tbdUTPase, 2) not binding to human dUTPase, 3) drug-like chemical property, and 4) nucleotide-like structure. The list included a well-known drug carbamazepine. These molecules were tested directly on *T. brucei*. If none of

these molecules showed any signs of killing the parasite, then a different approach would have been taken to find something that targets the essential dUTPase enzyme.

Out of the 13 molecules tested, molecule #4 was shown to significantly kill *T. brucei* with another molecule (#5) showing partial killing. 13 molecules is not a lot of candidates to screen through so for one to give the desired result was again very promising. Next, we tested whether molecule #4 was a dUTPase specific inhibitor, or whether its presence affected another pathway or essential enzyme leading to the parasite's cell death. Being able to purify our proteins of interest, allowed us to directly test if molecule #4 is indeed inhibit dUTPase activity. Both the PiPer Pyrophosphate Assay Kit and PCR-based dUTPase enzymatic activity assay, which are standard methods to test the activity of dUTPases in the presence of molecule #4. Although the results of the PiPer assay were inconclusive due to the failure of controls, the results of PCR-based assay showed all of the positive and negative controls were working properly. However, this assay showed that neither molecule #4 or #5 is an inhibitor of dUTPase.

There are a few different things that could be done to possibly achieve better results. Firstly, modifying the experiments that have already been done could provide us with our expected results. The AID system was used as a conditional knockdown method to be able to study the essential protein dUTPase. As stated, and shown in the results, the AID system was not very consistent when it came to growing cultures in the presence of auxin. Several times the survival rates and growth curves were not as expected due to the possible growth of suppressor mutations, which rendered the AID system ineffective. In our lab, the pTET system has been successfully used to create conditional knockouts. The endogenous yDUT1 could be under the control of a tetracycline inducible promoter (pTET). Human and *T. brucei* dUTPase genes

could be transformed into the cells and the expression of the endogenous *yDUT1* could be turned off, allowing for complementation to occur.

Another experiment that may be changed would be protein purification. Protein purification can be a rigorous process and does indeed take a significant amount of time to get the proper overexpression and washing conditions to get a valuable, pure purified protein. Revisiting the purification protocols and trying different overexpression inducers, protein tag, and washing buffers could most definitely result in a purer sample to be purified.

When the dUTPase genes were integrated into the yeast genome at the *HO* locus, the AID system no longer seemed to be properly functioning. Instead of adding the dUTPase genes at a different locus, the genes can be directly added to replace the endogenous *DUT1* gene. One of ways to accomplish this is to instead use a diploid yeast strain. In a diploid strain, there are two copies of *DUT1*. Either human or *T. brucei* dUTPase genes can be swapped out with one of the copies of the endogenous *DUT1* via homologous recombination and the yeast cell will still be viable because it still contains the other *DUT1* copy. Plasmids with the expression cassette for either *hDUT* or *tbdUTPase* can be transformed into the diploid cells. The diploid cells containing one copy of *yDUT1* gene and a plasmid-born *hDUT* or *tbdUTPase* gene can be induced to undergo sporulation, which results in a tetrad of four haploid spores [46]. These spores can then be separated via micromanipulation, and then grown in rich medium. If *hDUT* or *tbdUTPase* can functionally complement the loss of *yDut1*, some of the spores will contain the deletion at endogenous *DUT1* locus along with the plasmid. If functional complementation is not possible, no spores with the deletion at endogenous *DUT1* locus will be able to survive.

Another method to test for functional complementation is called plasmid shuffling. The purpose of plasmid shuffling is to introduce two plasmids to your Ura- and Leu- cell strain, one plasmid containing *WT yDUT1* with a *URA3* marker and the

second plasmid containing *hDUT* with a *LEU2* marker [47]. First, the strain is grown in rich media and transformed with the *WT yDUT1 URA3* plasmid and cells are selected for and grown in Ura-. The endogenous *DUT1* gene can at this point be deleted without loss of cell viability due to the plasmid expressed *DUT1*. The second *hDUT-LEU2* plasmid is then also transformed and then selected for in Ura- and Leu-. Colonies that grow should contain both plasmids. The colonies can be replica plated onto 5-FOA plates to select for cells that lost the *WT yDUT1-URA3* plasmid. If *hDUT* can functionally complement the loss of yeast *Dut1*, colonies containing only the *hDUT-LEU2* plasmid should be viable. The viable cells can then be further tested for complementation. The same experiments can be done with *tbdUTPase-LEU2* plasmid to test whether *T. brucei* dUTPase enzyme can functionally complement the yeast protein.

Lastly, we have directly showed that molecule #4 kills *T. brucei*. The best way to see how it is killing the cells is by directly studying it in *T. brucei*. Molecule #4 consists of a single S atom in its structure. A chemically synthetic form of this molecule could be generated using the radioactive isotope ^{35}S and then used to treat the parasite [48]. This synthetic molecule should be tracked where in the parasite it localizes to in order to see how the molecule might be affecting the viability of *T. brucei*. The ^{35}S can be tracked with various microscopy and autoradiography methods.

I was unable to show that the addition of human or *T. brucei* dUTPase can complement in the absence of the endogenous yeast dUTPase and failed to identify a *tbdUTPase*-specific ligand. However, through this project a single small molecule was found to kill *T. brucei* directly and have no effect on yeast. Since the dUTPase pathway is well studied, I believe it still holds promise in terms of having potential as a viable drug target to combat *T. brucei* infections. Furthermore, with the world adapting to computers and technology being involved more and more in all fields,

virtual drug screening has the potential to change the pharmaceutical industry. The results presented here show a promising method and provides an opportunity to pursue other scientific methods to potentially combat *T. brucei*.

Bibliography

- [1] Brun R., Blum J., Chappuis F., Burri C. (2010). Human African trypanosomiasis. *Lancet*, 375:148–159. doi: 10.1016/S0140-6736(09)60829-1.
- [2] Mitashi, P., Hasker, E., Lejon, V., Kande, V., Muyembe, J. J., Lutumba, P., Boelaert, M. (2012). Human African trypanosomiasis diagnosis in first-line health services of endemic countries, a systematic review. *PLoS Neglected Tropical Diseases*, 6(11), e1919. <https://doi.org/10.1371/journal.pntd.0001919>.
- [3] MacLean, L., Reiber, H., Kennedy, P. G., Sternberg, J. M. (2012). Stage progression and neurological symptoms in *Trypanosoma brucei rhodesiense* sleeping sickness: role of the CNS inflammatory response. *PLoS Neglected Tropical Diseases*, 6(10), e1857. <https://doi.org/10.1371/journal.pntd.0001857>.
- [4] Lejon, V., Ngoyi, D., Boelaert, M., Büscher, P. (2010). A CATT negative result after treatment for human African trypanosomiasis is no indication for cure. *PLoS Neglected Tropical Diseases*, 4(1): e590. <https://doi.org/10.1371/journal.pntd.0000590>.
- [5] Büscher, P., Cecchi, G., Jamonneau, V., Priotto, G. (2017). Human African trypanosomiasis. *Lancet*, 390(10110):2397–2409. doi: 10.1016/S0140-6736(17)31510-6.
- [6] Barry, J. D., McCulloch, R. (2001). Antigenic variation in trypanosomes: enhanced phenotypic variation in a eukaryotic parasite. *Advances in Parasitology*, 49, 1–70. [https://doi.org/10.1016/s0065-308x\(01\)49037-3](https://doi.org/10.1016/s0065-308x(01)49037-3).
- [7] Franco, J. R., Simarro, P. P., Diarra, A., Jannin, J. G. (2014). Epidemiology of human African trypanosomiasis. *Clinical Epidemiology*, 6, 257–275. <https://doi.org/10.2147/CLEP.S39728>.
- [8] Kennedy, P., Rodgers, J. (2019). Clinical and neuropathogenetic aspects of human African trypanosomiasis. *Frontiers in Immunology*, 10, 39. <https://doi.org/10.3389/fimmu.2019.00039>.

- [9] Barrett, M. P., Boykin, D. W., Brun, R., Tidwell, R. R. (2007). Human African trypanosomiasis: pharmacological re-engagement with a neglected disease. *British Journal of Pharmacology*, 152(8), 1155–1171. <https://doi.org/10.1038/sj.bjp.0707354>.
- [10] Voogd, T. E., Vansterkenburg, E. L., Wilting, J., Janssen, L. H. (1993). Recent research on the biological activity of suramin. *Pharmacological Reviews*, 45(2), 177–203.
- [11] Gibaud, S., Zirar, S. B., Mutzenhardt, P., Fries, I., Astier, A. (2005). Melarsoprol-cyclodextrins inclusion complexes. *International Journal of Pharmaceutics*, 306(1-2), 107–121. <https://doi.org/10.1016/j.ijpharm.2005.09.003>.
- [12] Shu, X., Liu, M., Lu, Z., Zhu, C., Meng, H., Huang, S., Zhang, X., Yi, C. (2018). Genome-wide mapping reveals that deoxyuridine is enriched in the human centromeric DNA. *Nature Chemical Biology*, 14(7), 680-687.
- [13] Owiti, N., Wei, S., Bhagwat, A. S., Kim, N. (2018). Unscheduled DNA synthesis leads to elevated uracil residues at highly transcribed genomic loci in *Saccharomyces cerevisiae*. *PLoS Genetics*, 14(7), e1007516. <https://doi.org/10.1371/journal.pgen.1007516>.
- [14] Bhagwat, A., Hao, W., Townes, J., Lee, H., Tang, H., Foster, P. (2016). Strand-biased cytosine deamination at the replication fork causes cytosine to thymine mutations in *Escherichia coli*. *Proceedings of the National Academy of Sciences*, 113. 201522325. [10.1073/pnas.1522325113](https://doi.org/10.1073/pnas.1522325113).
- [15] Owiti, N., Stokdyk, K., Kim, N. (2019). The etiology of uracil residues in the *Saccharomyces cerevisiae* genomic DNA. *Current Genetics*, 65(2), 393–399. <https://doi.org/10.1007/s00294-018-0895-8>.
- [16] Krokan, H., Drabløs, F., Slupphaug, G. (2002). Uracil in DNA – occurrence, consequences and repair. *Oncogene*, 21, 8935–8948. <https://doi.org/10.1038/sj.onc.1205996>.
- [17] Prorok, P., Alili, D., Saint-Pierre, C., Gasparutto, D., Zharkov, D., Ishchenko, A., Tudek, B., Sapparbaev, M. (2013). Uracil in duplex DNA is a substrate for the nucleotide incision

- repair pathway in human cells. *Proceedings of the National Academy of Sciences of the United States of America*, 110. 10.1073/pnas.1305624110.
- [18] Warner, H. R., Duncan, B. K., Garrett, C., Neuhard, J. (1981). Synthesis and metabolism of uracil-containing deoxyribonucleic acid in *Escherichia coli*. *Journal of Bacteriology*, 145(2), 687–695.
- [19] Hagenkort, A., Paulin, C., Desroses, M., Sarno, A., Wiita, E., Mortusewicz, O., Koolmeister, T., Loseva, O., Jemth, A. S., Almlöf, I., Homan, E., Lundbäck, T., Gustavsson, A. L., Scobie, M., Helleday, T. (2017). dUTPase inhibition augments replication defects of 5-Fluorouracil. *Oncotarget*, 8(14), 23713–23726. <https://doi.org/10.18632/oncotarget.15785>.
- [20] Bulgar, A. D., Weeks, L. D., Miao, Y., Yang, S., Xu, Y., Guo, C., Markowitz, S., Oleinick, N., Gerson, S. L., Liu, L. (2012). Removal of uracil by uracil DNA glycosylase limits pemetrexed cytotoxicity: overriding the limit with methoxyamine to inhibit base excision repair. *Cell Death & Disease*, 3(1), e252. <https://doi.org/10.1038/cddis.2011.135>.
- [21] Gadsden, M. H., McIntosh, E. M., Game, J. C., Wilson, P. J., Haynes, R. H. (1993). dUTP pyrophosphatase is an essential enzyme in *Saccharomyces cerevisiae*. *The EMBO Journal*, 12(11), 4425–4431.
- [22] Crosby, B., Prakash, L., Davis, H., Hinkle, D. C. (1981). Purification and characterization of a uracil-DNA glycosylase from the yeast, *Saccharomyces cerevisiae*. *Nucleic Acids Research*, 9(21), 5797–5809. <https://doi.org/10.1093/nar/9.21.5797>.
- [23] Wang, Z., Wu, X., Friedberg, E. (1997). Molecular mechanism of base excision repair of uracil-containing DNA in yeast cell-free extracts. *Journal of Biological Chemistry*, 272:24064–24071.
- [24] Tchigvintsev, A., Singer, A. U., Flick, R., Petit, P., Brown, G., Evdokimova, E., Savchenko, A., Yakunin, A. F. (2011). Structure and activity of the *Saccharomyces*

- cerevisiae* dUTP pyrophosphatase DUT1, an essential housekeeping enzyme. *The Biochemical Journal*, 437(2), 243–253. <https://doi.org/10.1042/BJ20110304>.
- [25] Hemsworth, G., Gonzalez-Pacanowska, D., Wilson, K. (2013). On the catalytic mechanism of dimeric dUTPases. *The Biochemical Journal*, 456:81–88. [https://doi:10.1042/BJ20130796](https://doi.org/10.1042/BJ20130796).
- [26] Wilson, P., Danenberg, P., Johnston, P., Lenz, H., Ladner, R. (2014). Standing the test of time: targeting thymidylate biosynthesis in cancer therapy. *Nature Reviews Clinical Oncology*, 11(5):282-298. [https://doi:10.1038/nrclinonc.2014.51](https://doi.org/10.1038/nrclinonc.2014.51).
- [27] Tanaka, S., Miyazawa-Onami, M., Iida, T., & Araki, H. (2015). iAID: an improved auxin-inducible degron system for the construction of a 'tight' conditional mutant in the budding yeast *Saccharomyces cerevisiae*. *Yeast*, 32(8), 567-581.
- [28] Zhao, Y. (2010). Auxin biosynthesis and its role in plant development. *Annual Review of Plant Biology*, 61, 49–64. <https://doi.org/10.1146/annurev-arplant-042809-112308>.
- [29] Papagiannakis, A., de Jonge, J., Zhang, Z., Heinemann, M. (2017). Quantitative characterization of the auxin-inducible degron: a guide for dynamic protein depletion in single yeast cells. *Scientific Reports*, 7, 4704. <https://doi.org/10.1038/s41598-017-04791-6>.
- [30] Cheng, T., Li, Q., Zhou, Z., Wang, Y., Bryant, S. H. (2012). Structure-based virtual screening for drug discovery: a problem-centric review. *The American Association of Pharmaceutical Scientists Journal*, 14(1), 133–141. <https://doi.org/10.1208/s12248-012-9322-0>.
- [31] Kenny, B. A., Bushfield, M., Parry-Smith, D. J., Fogarty, S., Treherne, J. M. (1998). The application of high-throughput screening to novel lead discovery. In *Progress in Drug Research* (pp. 245-269). Birkhäuser, Basel.
- [32] Batool, M., Ahmad, B., Choi, S. (2019). A structure-based drug discovery paradigm. *International Journal of Molecular Sciences*, 20(11), 2783. <https://doi.org/10.3390/ijms20112783>.

- [33] Lionta, E., Spyrou, G., Vassilatis, D. K., Cournia, Z. (2014). Structure-based virtual screening for drug discovery: principles, applications and recent advances. *Current Topics in Medicinal Chemistry*, 14(16), 1923–1938.
<https://doi.org/10.2174/1568026614666140929124445>.
- [34] *Glide*. Schrödinger Inc. <https://www.schrodinger.com/glide>.
- [35] Mol, C., Harris, J., McIntosh, E., Tainer, J. (1996). Human dUTP pyrophosphatase: uracil recognition by a beta hairpin and active sites formed by three separate subunits. *Structure*, 4(9):1077-1092. DOI: 10.1016/s0969-2126(96)00114-1.
- [36] Miyahara, S., Miyakoshi, H., Yokogawa, T., Chong, K. T., Taguchi, J., Muto, T., Endoh, K., Yano, W., Wakasa, T., Ueno, H., Takao, Y., Fujioka, A., Hashimoto, A., Itou, K., Yamamura, K., Nomura, M., Nagasawa, H., Shuto, S., Fukuoka, M. (2012). Discovery of a novel class of potent human deoxyuridine triphosphatase inhibitors remarkably enhancing the antitumor activity of thymidylate synthase inhibitors. *Journal of Medicinal Chemistry*, 55(7), 2970–2980. <https://doi.org/10.1021/jm201628y>.
- [37] Lipinski, C. (2004). Lead- and drug-like compounds: the rule-of-five revolution. *Drug Discovery Today: Technologies*, 1(4), 337–341.
<https://doi.org/10.1016/j.ddtec.2004.11.007>.
- [38] Dabrowski, S., Kiaer Ahring, B. (2003). Cloning, expression, and purification of the His6-tagged hyper-thermostable dUTPase from *Pyrococcus woesei* in *Escherichia coli*: application in PCR. *Protein Expression and Purification*, 31(1), 72–78.
[https://doi.org/10.1016/s1046-5928\(03\)00108-6](https://doi.org/10.1016/s1046-5928(03)00108-6).
- [39] Jensen, R., Sprague, G. F., Jr, Herskowitz, I. (1983). Regulation of yeast mating-type interconversion: feedback control of HO gene expression by the mating-type locus. *Proceedings of the National Academy of Sciences of the United States of America*, 80(10), 3035–3039. <https://doi.org/10.1073/pnas.80.10.3035>.
- [40] Harkiolaki, M., Dodson, E. J., Bernier-Villamor, V., Turkenburg, J. P., González-Pacanowska, D., Wilson, K. S. (2004). The crystal structure of *Trypanosoma cruzi*

- dUTPase reveals a novel dUTP/dUDP binding fold. *Structure*, 12(1), 41–53.
<https://doi.org/10.1016/j.str.2003.11.016>.
- [41] Alberts, B., Johnson, A., Lewis, J., Raff, M., Roberts, K., Walter, P. Molecular Biology of the Cell. 4th edition. New York: Garland Science; 2002. Protein Function. Available from: <https://www.ncbi.nlm.nih.gov/books/NBK26911/>.
- [42] Lertratanangkoon, K., Horning, M. G. (1982). Metabolism of carbamazepine. *Drug Metabolism and Disposition*, 10(1), 1-10.
- [43] Macdonald, R. L., McLean, M. J. (1986). Anticonvulsant drugs: mechanisms of action. *Advances in Neurology*, 44, 713–736.
- [44] Qaddouri, B., Guaadaoui, A., Bellirou, A., Hamal, A., Melhaoui, A., Brown, G. W., Bellaoui, M. (2011). The budding yeast "*Saccharomyces cerevisiae*" as a drug discovery tool to identify plant-derived natural products with anti-proliferative properties. *Evidence-based Complementary and Alternative Medicine*, 954140.
<https://doi.org/10.1093/ecam/nep069>.
- [45] Botstein, D., Chervitz, S. A., Cherry, J. M. (1997). Yeast as a model organism. *Science*, 277(5330), 1259–1260. <https://doi.org/10.1126/science.277.5330.1259>.
- [46] Morin, A., Moores, A. W., Sacher, M. (2009). Dissection of *Saccharomyces cerevisiae* asci. *Journal of Visualized Experiments*, (27), 1146. <https://doi.org/10.3791/1146>
- [47] Haase, M., Truong, D. M., & Boeke, J. D. (2019). Superloser: a plasmid shuffling vector for *saccharomyces cerevisiae* with exceedingly low background. *G3: Genes, Genomes, Genetics*, 9(8), 2699–2707. <https://doi.org/10.1534/g3.119.400325>
- [48] Alberts, B., Johnson, A., Lewis, J., Raff, M., Roberts, K., Walter, P. Molecular Biology of the Cell. 4th edition. New York: Garland Science; 2002. Visualizing Molecules in Living Cells. Available from: <https://www.ncbi.nlm.nih.gov/books/NBK26893/>.

Vita

Wahaj Ahmed Zuberi was born in Karachi, Pakistan to Jamil Ahmed and Sadaf Zuberi. He and two brothers, Hassan and Sameer, moved to Dallas, Texas in March 2003. After graduating high school in May 2013, he enrolled in the University of Texas at Arlington. There he received a Bachelor of Science in Biomedical Engineering with a double minor in Mathematics and Biochemistry in May 2017. After spending a year working full-time in industry for a company called Exact Diagnostics, he started graduate school at the University of Texas MD Anderson Cancer Center UTHealth Graduate School of Biomedical Sciences in August 2018 to pursue a master's degree.